

Deriving the Flavor Structure of the Standard Model from Trinification

August Koppers

Thesis Presented for Degree of Master in Science (30 Hp)

Supervisor: Roman Pasechnik



LUND
UNIVERSITY

Theoretical Particle Physics
Division of Particle & Nuclear Physics
Department of Physics
Lund University
Sweden
May 2024

Abstract

This thesis presents the derivation of the flavor structure of the Standard Model (SM) from the trinification model with an additional family symmetry. The trinification group is assumed to be broken in a single step to the electroweak gauge group. A low energy Effective Field Theory (EFT) is constructed and matched numerically at one loop level to the trinification model at high energies. The analysis focuses on an SM-like EFT with one Higgs-doublet, two scalar Lepto-Quarks (LQs), and one Vector-Like-Quark (VLQ) in the scalar potential. This is motivated by a numerical scan over the possible mass spectra. For parameter space points satisfying the correct mass spectrum at tree level, loop corrections are added, and the parameters are Renormalization Group (RG)-evolved down to the electroweak symmetry-breaking scale, at which predictions of the quark mass hierarchy and CKM matrix are compared to observations. The results reveal that the constructed EFT cannot accurately reproduce the correct SM quark masses, indicating the need for multiple Higgs particles to reproduce the observed SM, resulting in strong constraints on further considerations of this model.

Acknowledgments

Firstly, I would like to thank my supervisor Roman Pasechnik for his help throughout this project, his expertise with the subject proved invaluable throughout the project, and I've learned a lot under his guidance. I would also like to thank Werner Porod and António Morais for their helpful input in the project, especially Werner who helped with an attempted SARAH implementation. Moreover, I want to thank Hector Tiblom, whose code has been the basis of this analysis. Finally, I would also like to thank my family and friends for their support throughout this project.

Popular Science Description

It has long been known that the objects we interact with in everyday life are constituted by atoms. These atoms, in turn, consist of electrons, protons and neutrons, with the latter two being further composed of quarks. The electrons and quarks are known as elementary particles, meaning nothing constitutes them, which together with other elementary particles form the Standard Model of particle physics.

The Standard Model is, without doubt, one of the most successful descriptions of reality, describing the interactions of all elementary particles. Yet, despite its success, experimental contradictions questioning its completion have surfaced. This motivates the search for new models describing the experimentally verified part of the Standard Model, whilst solving its anomalies.

One such model that aims to both be consistent with the Standard Model and address its limitations is the trinification model, consisting of a larger symmetry group that is symmetric between left and right-handed particles. Studying the trinification model presents the opportunity to receive insight into many features of the elementary particles of the Standard Model, such as the origin of the large mass differences among the quarks, the existence of dark matter, and the observation of matter anti-matter asymmetry.

Contents

1	Introduction	1
1.1	Aim of thesis	2
2	Trinification model	3
2.1	Field content	3
2.1.1	Note on notation	4
2.2	Lagrangian	5
3	Symmetry breaking	8
3.1	Tadpole equations	8
3.2	Breaking to SM gauge group	9
4	Low-scale fields	11
4.1	Tree-level masses	12
4.1.1	Scalars	12
4.1.2	Gauge bosons	14
4.1.3	Fermions	15
5	Effective Field Theory	17
5.1	EFT fields and Lagrangian	17
5.2	Formalism of EFTs	19
5.3	EFT matching equations	20
5.4	Loop integrals	23
6	Matching to the Standard Model	26
6.1	RG evolution and β -functions	26
6.2	Electroweak symmetry breaking	26
6.3	Quark masses and CKM matrix	27
7	Numerical implementation	29
7.1	Tree level scan	29
7.2	One loop matching scan	30
8	Results and discussion	31
8.1	Improvements and outlook	34
9	Conclusion	35
A	Appendix: Tadpole equations	36
B	Appendix: EFT matching equations examples	36

Acronyms

CKM Cabibbo–Kobayashi–Maskawa

C(P) Charge(-Parity)

DOF Degrees Of Freedom

EFT Effective Field Theory

EW(SB) Electro-Weak (Symmetry-Breaking)

GUT Grand Unified Theory

LQ Lepto-Quark

MS Minimal Subtraction

$\overline{\text{MS}}$ Modified Minimal Subtraction

RG(E) Renormalization Group (Equation)

SM Standard Model

SVD Singular Value Decomposition

VEV Vacuum Expectation Value

VLQ Vector-Like-Quark

1 Introduction

The Standard Model (SM) of particle physics has proven to be one of the most successful descriptions of reality. Yet, discrepancies between measurements and theoretical predictions of the SM have been observed, such as the observed matter anti-matter asymmetry, neutrino masses, and the existence of dark matter. The SM also leaves many questions unanswered, such as the large hierarchy of the quark masses [1], which has led many physicists to believe the SM to be incomplete. Furthermore, the discovery of the Higgs boson, and the correctly predicted unification of the weak and electromagnetic forces into the Electro-Weak (EW) force, invigorated physicists to theorize of a Grand Unified Theory (GUT) that would unite the EW and the strong force. Many such models exist but none have been experimentally verified. One such model that potentially could explain many of the observed discrepancies and unify the fundamental forces (except gravity) is the trinification model.

The trinification model, first considered in 1984 in [2], is composed of a gauge group consisting of three $SU(3)$ groups: $SU(3)_L \times SU(3)_R \times SU(3)_C$, referring to left, right and color respectively. Originally an additional \mathbb{Z}_3 symmetry was also added, imposing the gauge couplings to unify at a GUT scale, making this a viable GUT theory. The trinification model has numerous advantages such as being flexible enough to allow for any masses and mixing angles for quarks and leptons [3]. In particular, the $SU(3)_R$ group allows for the inclusion of right-handed neutrinos, permitting neutrino masses. Additionally, the model incorporates extra Higgs-doublets allowing for additional CP-violation, potentially explaining the observed matter-antimatter asymmetry [4]. Another motivation for the study of the trinification model is the fact that it appears as a maximal subgroup of the exceptional Lie group E_6 , a group commonly used in GUT models due to it being anomaly-free [5, 6]. Furthermore, the trinification group also appears in the compactification of $E_8 \times E_8$ heterogenic string theories [4, 7]. This motivates the investigation of the trinification model structure from a theoretical point of view.

This thesis explores a specific variant of the trinification model. Firstly, the \mathbb{Z}_3 symmetry is not imposed, because this requires the energy scale, at which the EW and strong coupling constants are unified, to be very large. Hence, the imposition of the gauge couplings to unify is not considered in this model. The variation of the trinification gauge group considered is $[SU(3)]^3 \times SU(2)_F \times U(1)_F$, where $SU(2)_F \times U(1)_F$ represent an additional family symmetry, restricting the possible terms in the Lagrangian, with $SU(2)_F$ being a gauge symmetry and $U(1)_F$ being a global symmetry. Having both family doublets and singlets in the model results in, after the family symmetry is broken, three particles corresponding to the three generations in the SM. Since $[SU(3)]^3 \subset E_6$, this model can be viewed as an intermediate stage in a larger chain of broken symmetries starting from an even larger E_6 GUT theory. The additional family symmetries allow for the unification of gauge couplings above the trinification scale, motivating the view of the model considered in this thesis as a partial breaking step in a larger theory. This view is supported by [8], where an E_8 group is broken into a supersymmetric version of the gauge group considered in this thesis, which in turn is broken in several steps down to the SM.

To study how a model beyond the SM, such as the trinification model, would affect the physics of the SM, an Effective Field Theory (EFT), as a low-energy limit of the trinification theory is constructed and matched at one loop level. As usual in the SM,

at a given energy, the produced particles in a scattering event cannot have a total mass exceeding the input energy. Hence, adding a heavy particle to the SM would never be directly observed, nevertheless, it would appear as a virtual particle in interactions, indirectly affecting observables. In the trinification model, many such heavy particles are added, which cannot be observed at currently accessible energies. An EFT is constructed to examine how a model, such as the trinification model, would affect the observable phenomena of the SM, describing the impact of the high energy theory at lower energies. This is achieved by calculating effective couplings, defined as the sum of the tree level coupling plus all possible interactions with heavy particles only appearing in loops as virtual particles [9]. The resulting EFT can hence be designed to resemble the SM, but still depend on the parameters of the high energy theory.

A similar model to the one considered in this thesis has been studied at tree level in [10]. Consequently, the introductory sections describing the model will share many features. The analysis at tree level had difficulties accommodating the correct Cabibbo–Kobayashi–Maskawa (CKM) matrix and quark mass spectrum. Extending the analysis by matching the EFT at one loop order will provide deeper insight into how the predicted particles of the trinification model would influence the observable structures of the SM, such as the quark mass hierarchy and the CKM matrix.

In this thesis a trinification model, $[\text{SU}(3)]^3$, with the additional $\text{SU}(2)_F \times \text{U}(1)_F$ family gauge symmetry is considered. The fields, their representations, the Lagrangian, and accidental symmetries are described in sec. 2. The trinification group is broken in one step with the corresponding Vacuum Expectation Values (VEVs) and the remaining gauge and global symmetries are calculated in sec. 3. Subsequently, the field components are renamed; their charges under the new broken symmetry group, and their mass matrices are calculated in sec. 4. The EFT model is detailed in sec. 5, as well as the mathematical formalism of the matching procedure and calculations of loop integrals. In sec. 6, Renormalization Group (RG) evolution and EW symmetry breaking are described, as well as properties to compare between the matched EFT and the SM, such as quark masses and the CKM matrix. The EFT matching was implemented numerically by first finding parameters resulting in the correct tree level mass spectrum and adding loop corrections for respective points, described in sec. 7. The results of the numerical scan and the one loop matching are detailed in sec. 8, together with an outlook for further analysis of this model. Finally, sec. 9 concludes the method and results of the thesis.

1.1 Aim of thesis

This thesis aims to derive the flavor structure of the SM quarks as well as the mass hierarchy and CKM matrix, from the trinification model with an additional $\text{SU}(2)_F \times \text{U}(1)_F$ family symmetry. This is done by first assigning VEVs such that the $\text{SU}(3)_R$ and $\text{SU}(2)_F$ are completely broken, and $\text{SU}(3)_L$ is broken into $\text{SU}(2)_L$. Next, heavy fields are integrated out and an EFT is constructed and matched to the full theory at one loop level using a numerical implementation. The numerical computations are performed by first scanning the tree level mass spectrum and adding loop corrections to any point satisfying the EFT mass spectrum and parameter constraints. The matched EFT is then transformed, by RG evolution, to the energy scale of EW symmetry breaking, at which the Higgs mass parameter runs negative, giving mass to the SM quarks, and predictions of the analyzed model can be compared to observations.

2 Trinification model

The trinification model, as discussed in the introduction, is an attractive candidate for beyond the Standard Model model building, consisting of the gauge group:

$$SU(3)_C \times SU(3)_L \times SU(3)_R, \quad (2.1)$$

which is commonly used in GUT models, where the three gauge couplings are unified by a \mathbb{Z}_3 -symmetry, that cyclically permutes the $SU(3)$ groups. Even so, the model considered in this thesis is not a GUT model, but it still has a \mathbb{Z}_3 -symmetry reducing the number of model parameters. Additionally, a $SU(2)_F \times U(1)_F$ symmetry is imposed to further constrain the allowed terms in the Lagrangian. Here, the $U(1)_F$ symmetry added is an exact global group of the fermion sector, but is softly broken by terms in the scalar potential. Soft symmetry breaking refers to the symmetry being broken explicitly by quadratic or trilinear terms in the Lagrangian. That it is "soft" refers to the fact that the symmetry will only appear broken at lower energies and will in general not affect the running of any couplings. Thus, the gauge group considered in this work becomes:

$$SU(3)_C \times SU(3)_L \times SU(3)_R \times SU(2)_F \times \mathbb{Z}_3 \quad (2.2)$$

The Lagrangian that will be described in sec. 2.2, also contains two accidental symmetries: $U(1)_A$ and $U(1)_B$, the latter of which corresponds to the baryon charge which will remain unbroken, as will be shown in sec. 3.

In this section, the fields within the model, their representations and charges under the various symmetries, as well as the Lagrangian, for scalar, fermion, and gauge sectors, are defined.

2.1 Field content

The fundamental representation of the trinification group, $[SU(3)]^3$, is a **27**-plet. Thus, the fundamental representation of the gauge group given in eq. (2.2) can be decomposed into:

$$\mathbf{27}^i = \underbrace{(\mathbf{1}, \mathbf{3}, \bar{\mathbf{3}})^i}_{\tilde{L}^i, L^i} \oplus \underbrace{(\mathbf{3}, \bar{\mathbf{3}}, \mathbf{1})^i}_{\tilde{Q}_L^i, Q_L^i} \oplus \underbrace{(\bar{\mathbf{3}}, \mathbf{1}, \mathbf{3})^i}_{\tilde{Q}_R^i, Q_R^i}, \quad i = 1, 2, 3 \quad (2.3)$$

where the family index $i = (1, 2)$ is put into an $SU(2)_F$ doublet, and $i = 3$ is placed into a singlet. The bar denotes the field being in the anti-fundamental representation of the group, defined as the complex conjugate of the representation.

Adding scalars and left-handed Weyl fermions into these representations we have the scalars, denoted by a tilde, $\tilde{L}^i, \tilde{Q}_L^i, \tilde{Q}_R^i$; and the fermions, L^i, Q_L^i, Q_R^i ; with their representations shown in eq. (2.3). The fields L^i, Q_L^i , and Q_R^i denote lepton, left-handed quarks, and left-handed anti-quarks (charge conjugated right-handed Weyl-spinors) respectively.

However, to avoid a theoretical inconsistency known as the Witten anomaly, we need to introduce additional particles. The Witten anomaly arises for (dimension four) gauge theories with an odd number of $SU(2)$ fermion doublets [11]. Hence, we add one additional $SU(2)_F$ fermion doublet, N^I ($I = 1, 2$), and their corresponding scalar fields, \tilde{N}^I , both of which are put into singlets in the other gauge groups. Lastly, an additional scalar singlet is added, \tilde{S} , to give mass to the N^I fermions by \tilde{S} acquiring a VEV.

Thus, the model contains the following left-handed Weyl fermions: L^i, Q_L^i, Q_R^i and N^I ; the scalars: $\tilde{L}^i, \tilde{Q}_L^i, \tilde{Q}_R^i, \tilde{N}^I$ and \tilde{S} ; and the gauge bosons: G_C, G_L, G_R and G_F . A summary of all the high-scale fields and their representations is given in tab. 1.

Table 1: Summary of fields in high-scale model and which representation of the gauge group, eq. (2.2), they belong to.

	SU(3) _C	SU(3) _L	SU(3) _R	SU(2) _F
Fermions & Scalars				
L^I, \tilde{L}^I	1	3	$\bar{\mathbf{3}}$	2
L^3, \tilde{L}^3	1	3	$\bar{\mathbf{3}}$	1
Q_L^I, \tilde{Q}_L^I	3	$\bar{\mathbf{3}}$	1	2
Q_L^3, \tilde{Q}_L^3	3	$\bar{\mathbf{3}}$	1	1
Q_R^I, \tilde{Q}_R^I	$\bar{\mathbf{3}}$	1	3	2
Q_R^3, \tilde{Q}_R^3	3	1	3	1
N^I, \tilde{N}^I	1	1	1	2
\tilde{S}	1	1	1	1
Gauge Bosons				
G_C	8	1	1	1
G_L	1	8	1	1
G_R	1	1	8	1
G_F	1	1	1	3

The Lagrangian, described in sec. 2.2, also possess two accidental symmetries, $U(1)_A$ and $U(1)_B$, the latter of which gives rise to a baryon number conservation and will remain unbroken, as seen in sec. 3. The fields are assigned charges under the $U(1)_A$, $U(1)_B$, and $U(1)_F$ symmetries, similar to a model considered in [7]. This charge assignment is shown in tab. 2.

Table 2: Charge assignment under the accidental symmetries, $U(1)_A$ and $U(1)_B$, as well as the softly broken $U(1)_F$ symmetry.

Field Component	$U(1)_A$	$U(1)_B$	$U(1)_F$
L^I, \tilde{L}^I	1	0	-1/2
L^3, \tilde{L}^3	1	0	1
Q_L^I, \tilde{Q}_L^I	-1/2	1/3	-1/2
Q_L^3, \tilde{Q}_L^3	-1/2	1/3	1
Q_R^I, \tilde{Q}_R^I	-1/2	-1/3	-1/2
Q_R^3, \tilde{Q}_R^3	-1/2	-1/3	1
N^I, \tilde{N}^I	0	0	-1/2
\tilde{S}	0	0	1

2.1.1 Note on notation

The fields of the trinification model can have both fundamental and anti-fundamental components. In this thesis, indices in the fundamental representation are written as upper indices, and anti-fundamental as lower indices. The fields are written in the form

$(\tilde{L}^i)_r^l$ where the indices outside the parentheses are the trification group indices (note from tab. 1 that l and r are in the $\mathbf{3}$ and $\bar{\mathbf{3}}$ respectively). The indices used will have the following conventions, lower case indices i, k, l, r, c will range from 1 to 3, the index a will take values from 1 to 8, and the upper case indices I, J, L, R will take the values 1 and 2.

The components of the fields can be written in a matrix representation, where the upper (fundamental) index will indicate the row and the lower (anti-fundamental) index indicates the column of the matrix. For instance, $(\tilde{L}^i)_r^l$ is represented by a 3×3 matrix for each i .

Lastly, to shorten the notation of the Lagrangian the discrete \mathbb{Z}_3 group, defined to cyclically permute the fields is introduced:

$$\begin{array}{cccc}
(L^i)_r^l & \xrightarrow{\mathbb{Z}_3} & (Q_L^i)_l^c & & (\tilde{L}^i)_r^l & \xrightarrow{\mathbb{Z}_3} & (\tilde{Q}_L^i)_l^c & & G_L & \xrightarrow{\mathbb{Z}_3} & G_C & & g_L & \xrightarrow{\mathbb{Z}_3} & g_C \\
& \swarrow \mathbb{Z}_3 & & \searrow \mathbb{Z}_3 & & \swarrow \mathbb{Z}_3 & & \searrow \mathbb{Z}_3 & & \swarrow \mathbb{Z}_3 & & \searrow \mathbb{Z}_3 & & \swarrow \mathbb{Z}_3 & & \searrow \mathbb{Z}_3 \\
& & (Q_R^i)_c^r & & & & (\tilde{Q}_R^i)_c^r & & & & G_R & & & & g_R
\end{array}$$

2.2 Lagrangian

The Lagrangian used is the most general realizable Lagrangian invariant under the gauge group, eq. (2.2), where the \mathbb{Z}_3 symmetry is imposed to reduce the number of parameters.

The scalar potential is divided up as:

$$V = V_1 + V_2 + V_3 + V_4 + V_5 + V_6 \quad (2.4)$$

where V_1 contains all mass- and quartic bi-triplet self-interaction terms; V_2 contains all quartic interactions between the bi-triplets; V_3 contains all trilinear terms between the bi-triplet fields; V_4 contains all \tilde{N}^I , \tilde{S} masses and interactions; V_5 contains all quartic terms between a bi-triplet and either \tilde{N}^I or \tilde{S} ; and V_6 contains all trilinear terms between \tilde{N}^I , \tilde{S} , and one bi-triplet.

$$\begin{aligned}
V_1 = & \mu_1^2 (\tilde{L}^I)_r^l (\tilde{L}_I^*)_l^r + \mu_2^2 (\tilde{L}^3)_r^l (\tilde{L}_3^*)_l^r + \lambda_1 [(\tilde{L}^I)_r^l (\tilde{L}_I^*)_l^r]^2 \\
& + \lambda_2 (\tilde{L}^I)_r^l (\tilde{L}_I^*)_l^r (\tilde{L}^3)_{r'}^{l'} (\tilde{L}_3^*)_{l'}^{r'} + \lambda_3 [(\tilde{L}^3)_r^l (\tilde{L}_3^*)_l^r]^2 \\
& + \lambda_4 (\tilde{L}^I)_r^l (\tilde{L}^J)_{r'}^{l'} (\tilde{L}_J^*)_l^r (\tilde{L}_I^*)_{l'}^{r'} + \lambda_5 (\tilde{L}^I)_r^l (\tilde{L}^3)_{r'}^{l'} (\tilde{L}_3^*)_l^r (\tilde{L}_I^*)_{l'}^{r'} \\
& + \lambda_6 (\tilde{L}^I)_r^l (\tilde{L}^J)_{r'}^{l'} (\tilde{L}_I^*)_l^r (\tilde{L}_J^*)_{l'}^{r'} + \lambda_7 (\tilde{L}^I)_r^l (\tilde{L}^3)_{r'}^{l'} (\tilde{L}_I^*)_l^r (\tilde{L}_3^*)_{l'}^{r'} \\
& + \lambda_8 (\tilde{L}^3)_r^l (\tilde{L}^3)_{r'}^{l'} (\tilde{L}_3^*)_l^r (\tilde{L}_3^*)_{l'}^{r'} + \lambda_9 (\tilde{L}^I)_r^l (\tilde{L}^J)_{r'}^{l'} (\tilde{L}_J^*)_l^r (\tilde{L}_I^*)_{l'}^{r'} \\
& + \lambda_{10} (\tilde{L}^I)_r^l (\tilde{L}^3)_{r'}^{l'} (\tilde{L}_3^*)_l^r (\tilde{L}_I^*)_{l'}^{r'} + (\mathbb{Z}_3 \text{ permutations})
\end{aligned} \quad (2.5)$$

$$\begin{aligned}
V_2 = & \alpha_1 (\tilde{L}^I)_r^l (\tilde{L}_I^*)_l^r (\tilde{Q}_L^J)_l^c (\tilde{Q}_{LJ}^*)_c^l + \alpha_2 (\tilde{L}^3)_r^l (\tilde{L}_3^*)_l^r (\tilde{Q}_L^I)_l^c (\tilde{Q}_{LI}^*)_c^l \\
& + \alpha_3 (\tilde{L}^I)_r^l (\tilde{L}_I^*)_l^r (\tilde{Q}_L^3)_l^c (\tilde{Q}_{L3}^*)_c^l + \alpha_4 (\tilde{L}^3)_r^l (\tilde{L}_3^*)_l^r (\tilde{Q}_L^I)_l^c (\tilde{Q}_{L3}^*)_c^l \\
& + \alpha_5 (\tilde{L}^I)_r^l (\tilde{L}_J^*)_l^r (\tilde{Q}_L^I)_l^c (\tilde{Q}_{LJ}^*)_c^l \\
& + \alpha_6 \left[(\tilde{L}^3)_r^l (\tilde{L}_I^*)_l^r (\tilde{Q}_L^I)_l^c (\tilde{Q}_{L3}^*)_c^l + (\tilde{L}^I)_r^l (\tilde{L}_3^*)_l^r (\tilde{Q}_L^3)_l^c (\tilde{Q}_{LI}^*)_c^l \right] \\
& + \alpha_7 (\tilde{L}^I)_r^l (\tilde{L}_I^*)_l^r (\tilde{Q}_L^J)_l^c (\tilde{Q}_{LJ}^*)_c^l + \alpha_8 (\tilde{L}^3)_r^l (\tilde{L}_3^*)_l^r (\tilde{Q}_L^I)_l^c (\tilde{Q}_{L3}^*)_c^l \\
& + \alpha_9 (\tilde{L}^I)_r^l (\tilde{L}_I^*)_l^r (\tilde{Q}_L^3)_l^c (\tilde{Q}_{L3}^*)_c^l + \alpha_{10} (\tilde{L}^3)_r^l (\tilde{L}_3^*)_l^r (\tilde{Q}_L^I)_l^c (\tilde{Q}_{L3}^*)_c^l \\
& + \alpha_{11} (\tilde{L}^I)_r^l (\tilde{L}_J^*)_l^r (\tilde{Q}_L^J)_l^c (\tilde{Q}_{LJ}^*)_c^l \\
& + \alpha_{12} \left[(\tilde{L}^3)_r^l (\tilde{L}_I^*)_l^r (\tilde{Q}_L^I)_l^c (\tilde{Q}_{L3}^*)_c^l + (\tilde{L}^I)_r^l (\tilde{L}_3^*)_l^r (\tilde{Q}_L^3)_l^c (\tilde{Q}_{LI}^*)_c^l \right] \\
& + (\mathbb{Z}_3 \text{ permutations})
\end{aligned} \tag{2.6}$$

$$V_3 = \epsilon_{IJ} \left[\gamma_1 (\tilde{L}^I)_r^l (\tilde{Q}_L^J)_l^c (\tilde{Q}_R^3)_c^r + \gamma_2 (\tilde{L}^I)_r^l (\tilde{Q}_L^3)_l^c (\tilde{Q}_R^J)_c^r + \gamma_3 (\tilde{L}^3)_r^l (\tilde{Q}_L^I)_l^c (\tilde{Q}_R^J)_c^r \right] + \text{c.c} \tag{2.7}$$

$$V_4 = \mu_3^2 \tilde{N}^I \tilde{N}_I^* + \mu_4^2 \tilde{S} \tilde{S}^* + \frac{\eta^2}{2} (\tilde{S}^2 + \tilde{S}^{*2}) + \chi_1 [\tilde{N}^I \tilde{N}_I^*]^2 + \chi_2 [\tilde{S} \tilde{S}^*]^2 + \chi_3 \tilde{N}^I \tilde{N}_I^* \tilde{S} \tilde{S}^* \tag{2.8}$$

$$\begin{aligned}
V_5 = & \beta_1 (\tilde{L}^I)_r^l (\tilde{L}_I^*)_l^r \tilde{N}^J \tilde{N}_J^* + \beta_2 (\tilde{L}^I)_r^l (\tilde{L}_J^*)_l^r \tilde{N}^J \tilde{N}_I^* + \beta_3 (\tilde{L}^3)_r^l (\tilde{L}_3^*)_l^r \tilde{N}^I \tilde{N}_I^* \\
& + \beta_4 (\tilde{L}^I)_r^l (\tilde{L}_I^*)_l^r \tilde{S} \tilde{S}^* + \beta_5 (\tilde{L}^3)_r^l (\tilde{L}_3^*)_l^r \tilde{S} \tilde{S}^* + (\mathbb{Z}_3 \text{ permutations})
\end{aligned} \tag{2.9}$$

$$\begin{aligned}
V_6 = & \gamma_4 \tilde{S} \tilde{N}^I \tilde{N}_I^* + \gamma_5 \tilde{S} (\tilde{L}^I)_r^l (\tilde{L}_I^*)_l^r + \gamma_6 \tilde{S} (\tilde{L}^3)_r^l (\tilde{L}_3^*)_l^r + \gamma_7 \epsilon_{IJ} \tilde{N}^I (\tilde{L}^J)_r^l (\tilde{L}_3^*)_l^r \\
& + \text{c.c} + (\mathbb{Z}_3 \text{ permutations})
\end{aligned} \tag{2.10}$$

The Lagrangian of the fermionic sector is given by:

$$\begin{aligned}
\mathcal{L}_{\text{Yukawa}} = & - \epsilon_{IJ} \left[y_1 (\tilde{L}^I)_r^l (Q_L^J)_l^c (Q_R^3)_c^r + y_2 (\tilde{L}^I)_r^l (Q_L^3)_l^c (Q_R^J)_c^r + y_3 (\tilde{L}^3)_r^l (Q_L^I)_l^c (Q_R^J)_c^r \right. \\
& \left. + y_4 \tilde{S} N^I N^J \right] + \text{c.c} + (\mathbb{Z}_3 \text{ permutations}),
\end{aligned} \tag{2.11}$$

where the spin indices are implicitly being contracted over the Levi-Civita tensor.

The kinetic part of the Lagrangian, describing gauge boson interaction, is given by:

$$\begin{aligned}
\mathcal{L}_{\text{Gauge}} = & \left[\mathcal{D}_\mu (\tilde{L}^i)_r^l \right] \left[\mathcal{D}^\mu (\tilde{L}_i^*)_l^r \right] + \left[\mathcal{D}_\mu \tilde{N}^I \right] \left[\mathcal{D}^\mu \tilde{N}_I^* \right] + \left[\mathcal{D}_\mu \tilde{S} \right] \left[\mathcal{D}^\mu \tilde{S}^* \right] \\
& + (L^i)_r^l \not{D} (L_i^*)_l^r + N^I \not{D} N_I^* + S \not{D} S^* \\
& + \frac{1}{2} G_{L\mu\nu}^a G_L^{a\mu\nu} + \frac{1}{2} G_{R\mu\nu}^a G_R^{a\mu\nu} + \frac{1}{2} G_{C\mu\nu}^a G_C^{a\mu\nu} + \frac{1}{2} G_{F\mu\nu}^i G_F^{i\mu\nu} + (\mathbb{Z}_3 \text{ permutations}),
\end{aligned} \tag{2.12}$$

where the covariant derivative for the given gauge group for \tilde{L}^i is given by:

$$\mathcal{D}_\mu = \partial_\mu + ig_L T_L^a G_{L\mu}^a - ig_R T_R^a G_{R\mu}^a + ig_F T_F^a G_{F\mu}^a, \tag{2.13}$$

and similarly for \tilde{Q}_L and \tilde{Q}_R , with appropriate generators and minus signs. However, $\mathcal{D}_\mu \tilde{N}^I$ and $\mathcal{D}_\mu \tilde{S}$ would only contain the $SU(2)_F$ variation due to them being singlets in $SU(3)_L$ and $SU(3)_R$. And $G_{L\mu\nu}^a$ denote the field strength tensor of the $SU(3)_L$ gauge group, defined as:

$$G_{L\mu\nu}^a = \partial_\mu G_{L\nu}^a - \partial_\nu G_{L\mu}^a + g_L f^{abc} G_{L\mu}^b G_{L\nu}^c \quad (2.14)$$

and $G_{R\mu\nu}^a$, $G_{F\mu\nu}^a$ and $G_{C\mu\nu}^a$ are defined equivalently, with f^{abc} in eq. (2.14) being the structure constants of the corresponding gauge group.

Altogether, the parameters of the high-scale model are the 5 mass-parameters $\mu_{1,\dots,4}, \eta$, 7 trilinear scalar couplings $\gamma_{1,\dots,7}$, 4 Yukawa couplings $y_{1,\dots,4}$, and 30 quartic scalar couplings $\lambda_{1,\dots,10}, \alpha_{1,\dots,12}, \chi_{1,2,3}, \beta_{1,\dots,5}$.

3 Symmetry breaking

To arrive at a model consistent with the SM at lower energies the high rank of the trification group needs to be reduced. This is achieved by spontaneous symmetry breaking which also gives rise to massive gauge bosons, fermions, and scalars.

The $U(1)_F$ symmetry is softly broken, by the trilinear terms in V_6 , eq. (2.10). The energy scale at which this occurs is taken to be above the breaking of the trification group itself. Therefore, the $U(1)_F$ will be considered broken throughout the rest of the thesis.

Writing the field-components in matrix form, using the notation described in sec. 2.1.1, the VEVs that break the gauge group, eq. (2.2), down to a SM-like gauge group are

$$\begin{aligned} \langle \tilde{L}^1 \rangle &= \frac{1}{\sqrt{2}} \begin{pmatrix} 0 & 0 & 0 \\ 0 & 0 & 0 \\ 0 & \omega & 0 \end{pmatrix}, & \langle \tilde{L}^2 \rangle &= \frac{1}{\sqrt{2}} \begin{pmatrix} 0 & 0 & 0 \\ 0 & 0 & 0 \\ 0 & 0 & f \end{pmatrix}, & \langle \tilde{L}^3 \rangle &= \frac{1}{\sqrt{2}} \begin{pmatrix} 0 & 0 & 0 \\ 0 & 0 & 0 \\ 0 & 0 & p \end{pmatrix}, \\ \langle \tilde{N} \rangle &= \frac{1}{\sqrt{2}} \begin{pmatrix} \rho \\ 0 \end{pmatrix}, & \langle \tilde{S} \rangle &= \frac{w}{\sqrt{2}} \end{aligned} \quad (3.1)$$

Without a loss of generality, the VEVs ω, f, p, ρ and w are taken to be real and positive. Similar to the SM Higgs mechanism, scalars that acquire a VEV must have a corresponding potential with a minimum away from the origin. To impose this condition, the mass parameters of the fields acquiring VEVs must be negative, $\mu_{1,2,3,4}^2 < 0$.

This section details a one-step breaking scheme of the trification group to the SM gauge group, the minimization conditions of the scalar potential, known as tadpole equations, and the calculation of the new unbroken symmetries.

3.1 Tadpole equations

Tadpole equations are minimization conditions of the scalar potential with respect to the fields. This is to ensure that the VEVs are expanded around a minimum, mathematically it is written as:

$$\left. \frac{\partial V}{\partial \phi_j} \right|_{\phi_j = \langle \phi_j \rangle} = 0 \quad , \quad (3.2)$$

where $\langle \phi_j \rangle$ is the VEVs. In the SM the minimization condition is used to solve for the VEV in terms of other parameters of the model. Yet, in this thesis, the VEV scales are treated as inputs. Instead, the five VEVs, in eq. (3.1), give five minimization conditions used to eliminate the variables $\mu_1, \mu_2, \mu_3, \mu_4$ and γ_7 . The expression for these variables are given in Appendix A.

Mathematically, these minimization conditions ensure there are no linear terms in the Lagrangian, that is, a field never appears by itself. These linear terms would give rise to Feynman diagrams with a single external leg,



$$\text{-----} \bigcirc \quad (3.3)$$

referred to as tadpole diagrams [12].

3.2 Breaking to SM gauge group

The VEVs in eq. (3.1) can be written more compactly in terms of Kronecker-delta functions:

$$\langle (\tilde{L}^i)_r \rangle = \frac{1}{\sqrt{2}} \delta_3^l \left(\omega \delta_r^2 \delta_1^i + (f \delta_2^i + p \delta_3^i) \delta_r^3 \right). \quad (3.4)$$

Using the notation: $T^a = \lambda^a/2$, where λ^a are the Gell-Mann matrices, the generators of SU(3), the generators of SU(2) are written as the first three SU(3) generators, $T^k = T^{1,2,3}$, and the U(1)_A generator is given by T_A , and a constant number. A general transformation of the \tilde{L}^i fields, considering the gauge group, eq. (2.2), can then be written as:

$$\delta(\tilde{L}^i)_r = i\omega_L^a (T_L^a)_r^l (\tilde{L}^i)_r - i\omega_R^a (T_R^a)_r^{r'} (\tilde{L}^i)_{r'}^l + i\omega_F^k (T_F^k)_i^i (\tilde{L}^i)_r + i\omega_A (T_A) (\tilde{L}^i)_r \quad . \quad (3.5)$$

The minus sign for the SU(3)_R variation is due to \tilde{L}^i belonging to the anti-fundamental representation of this group. No variation with respect to SU(3)_C appear in eq. (3.5), due to \tilde{L}^I being a color singlet. Moreover, no U(1)_B appears due to \tilde{L}^i not being charged under this symmetry. Finally, considering that \tilde{L}^i has charge one under the U(1)_A transformations we can set (T_A) to unity.

In order to leave the vacuum invariant after expanding around the new minimum, the variation of the VEVs must vanish, $\delta \langle (\tilde{L}^i)_r \rangle = 0$. Combining eqs. (3.4) and (3.5) we get

$$\begin{aligned} \delta \langle (\tilde{L}^i)_r \rangle &= \frac{i}{\sqrt{2}} \left[\omega_L^a (T_L^a)_3^l \left(\omega \delta_r^2 \delta_1^i + (f \delta_2^i + p \delta_3^i) \delta_r^3 \right) - \omega_R^a \delta_3^l \left(\omega (T_R^a)_r^2 \delta_1^i + (T_R^a)_r^3 (f \delta_2^i + p \delta_3^i) \right) \right. \\ &\quad \left. + \omega_F^k \delta_3^l \left(\omega (T_F^k)_1^i \delta_r^2 + f (T_F^k)_2^i \delta_r^3 + p (T_F^k)_3^i \delta_r^3 \right) + \omega_A \delta_3^l \left(\omega \delta_r^2 \delta_1^i + (f \delta_2^i + p \delta_3^i) \delta_r^3 \right) \right] \\ &= 0 \quad . \end{aligned} \quad (3.6)$$

Using that $(T_F^k)_3^i = 0$ this can be written as

$$\begin{aligned} 0 &= \omega_L^a (T_L^a)_3^l \left(\omega \delta_r^2 \delta_1^i + (f \delta_2^i + p \delta_3^i) \delta_r^3 \right) - \omega_R^a \delta_3^l \left(\omega (T_R^a)_r^2 \delta_1^i + (T_R^a)_r^3 (f \delta_2^i + p \delta_3^i) \right) \\ &\quad + \omega_F^k \delta_3^l \left(\omega (T_F^k)_1^i \delta_r^2 + f (T_F^k)_2^i \delta_r^3 \right) + \omega_A \delta_3^l \left(\omega \delta_r^2 \delta_1^i + (f \delta_2^i + p \delta_3^i) \delta_r^3 \right) . \end{aligned} \quad (3.7)$$

Considering all combinations i, l, r , and imposing $\omega_L^a, \omega_R^a, \omega_F^k$ and ω_A to be real, we find which generators that are broken by the VEVs. For example, considering $i = l = r = 3$, eq. (3.7) reduces to

$$0 = \omega_L^a (T_L^a)_3^3 p - \omega_R^a (T_R^a)_3^3 p + \omega_F^k \left(\underbrace{(T_F^k)_1^3}_{=0} \omega + \underbrace{(T_F^k)_2^3}_{=0} f \right) + \omega_A p = \omega_L^a (T_L^a)_3^3 p - \omega_R^a (T_R^a)_3^3 p + \omega_A p$$

From the Gell-Mann matrices we have that $(T^a)_3^3 = -\frac{\delta_3^a}{\sqrt{3}}$, summing over a gives

$$\Rightarrow -\omega_L^8 \frac{1}{\sqrt{3}} + \omega_R^8 \frac{1}{\sqrt{3}} + \omega_A = 0.$$

Similarly for other combinations, we arrive at

$$\omega_L^{4,\dots,7} = \omega_R^{1,2,4,\dots,7} = \omega_F^{1,2,3} = 0, \quad (3.8)$$

$$\omega_R^3 - \sqrt{3}\omega_R^8 = 0, \quad (3.9)$$

$$\omega_L^8 - \omega_R^8 - \sqrt{3}\omega_A = 0. \quad (3.10)$$

From this we conclude that the generators $T_L^{4,\dots,7} = T_R^{1,2,4,\dots,7} = T_F^{1,2,3}$ are broken.

The generators T_L^8 , T_R^8 , T_R^3 and T_A are constrained by eq. (3.9) and eq. (3.10), the remaining unbroken generators must be a linear combination of these, giving rise to two independent unbroken U(1) generators, one of which will correspond to the hypercharge U(1)_Y. Considering a general transformation of T_L^8 , T_R^8 , T_R^3 and T_A , and using the derived constraints to eliminate $\omega_R^3 = \sqrt{3}\omega_R^8$ and $\omega_A = \frac{1}{\sqrt{3}}(\omega_L^8 - \omega_R^8)$, we get

$$\omega_L^8 T_L^8 + \omega_R^8 T_R^8 + \omega_R^3 T_R^3 + \omega_A T_A = \omega_L^8 T_L^8 + \omega_R^8 T_R^8 + \sqrt{3}\omega_R^8 T_R^3 + \frac{1}{\sqrt{3}}(\omega_L^8 - \omega_R^8) T_A. \quad (3.11)$$

Wanting to find a generator corresponding to hypercharge we choose to define,

$$\omega_L^8 \equiv -\frac{1}{\sqrt{3}}(\omega_Y + 4\omega_T), \quad \omega_R^8 \equiv \frac{1}{\sqrt{3}}(\omega_T - \omega_Y),$$

eq. (3.11) then becomes,

$$\begin{aligned} & \frac{\omega_Y}{\sqrt{3}} \left((-T_L^8 - T_R^8) - \sqrt{3}T_R^3 + T_A \cdot 0 \right) + \frac{\omega_T}{\sqrt{3}} \left(-4T_L^8 + \sqrt{3}T_R^8 + T_R^3 - \frac{4}{\sqrt{3}}T_A + \frac{1}{\sqrt{3}}T_A \right) = \\ & = \omega_Y \underbrace{\left(-\frac{1}{\sqrt{3}}(T_L^8 + T_R^8) - T_R^3 \right)}_{\equiv T_Y} + \omega_T \underbrace{\left(-\frac{4}{\sqrt{3}}T_L^8 - \frac{5}{3}T_A + T_R^8 - \frac{1}{\sqrt{3}}T_R^3 \right)}_{\equiv T_T}. \end{aligned} \quad (3.12)$$

Hence, we have found the generators T_Y and T_T :

$$T_Y = -\frac{1}{\sqrt{3}}(T_L^8 + T_R^8) - T_R^3, \quad T_T = -\frac{1}{\sqrt{3}}(4T_L^8 + T_R^3) - \frac{5}{3}T_A + T_R^8, \quad (3.13)$$

where T_T depends on T_A which generates a global symmetry, hence T_T must also be global.

The remaining unbroken generators are $T_L^{1,2,3}$, which are the generators of SU(2), therefore we have broken $SU(3)_L \rightarrow SU(2)_L$. Hence, the total breaking of the symmetry group can be written as:

$$\begin{aligned} & [SU(3)_C \times SU(3)_L \times SU(3)_R \times SU(2)_F] \times \{U(1)_F \times U(1)_A \times U(1)_B\} \\ & \quad \downarrow \\ & [SU(3)_C \times SU(2)_L \times U(1)_Y] \times \{U(1)_T \times U(1)_B\} \end{aligned} \quad (3.14)$$

where square brackets [...] denote gauge symmetries and curly ones {...} denote global symmetries.

4 Low-scale fields

After spontaneous symmetry breaking the new gauge group is described by eq. (3.14). In this section new names for the components of the high-scale fields are given, their quantum numbers are calculated, as well as the masses of all scalar, fermion, and gauge fields.

The components of the trinification fields are renamed, with the doublets denoting the leftover $SU(2)_L$ doublets, and neglecting any $SU(3)_C$ index as it is not broken. The components that receive a VEV, $(\tilde{L}^i)_2^3$ and $(\tilde{L}^i)_3^3$, are expanded into CP even and CP odd components, then the scalar fields are given by:

$$\tilde{L}^i = \begin{pmatrix} \begin{pmatrix} H_{d,1} \\ H_{d,2} \end{pmatrix}^i & \begin{pmatrix} H_{u,1} \\ H_{u,2} \end{pmatrix}^i & \begin{pmatrix} \tilde{\nu}_L \\ \tilde{e}_L \end{pmatrix}^i \\ \tilde{e}_R^i & (\tilde{L}^i)_2^3 & (\tilde{L}^i)_3^3 \end{pmatrix}, \quad \text{with :} \quad \begin{aligned} (\tilde{L}^i)_2^3 &= \frac{1}{\sqrt{2}} (\delta_1^i \omega + \tilde{\nu}_R^i + i\tilde{\nu}'^i) \\ (\tilde{L}^i)_3^3 &= \frac{1}{\sqrt{2}} (\delta_2^i f + \delta_3^i p + \tilde{\Phi}^i + i\tilde{\Phi}'^i) \end{aligned}$$

$$\tilde{Q}_L^i = \left(\begin{pmatrix} \tilde{d}_L & \tilde{u}_L & \tilde{D}_L \end{pmatrix} \right)^i, \quad \tilde{Q}_R^i = \begin{pmatrix} \tilde{u}_R \\ \tilde{d}_R \\ \tilde{D}_R \end{pmatrix}^i.$$

The \tilde{N}^I , and \tilde{S} fields are also expanded around their VEVs as:

$$\tilde{N}^I = \frac{1}{\sqrt{2}} (\delta_1^I \rho + \tilde{n}^I + i\tilde{n}'^I), \quad \tilde{S} = \frac{1}{\sqrt{2}} (w + \tilde{s} + i\tilde{s}'). \quad (4.2)$$

The fermion fields are given as:

$$L^i = \begin{pmatrix} \begin{pmatrix} \mathcal{E}_R \\ \mathcal{N}_R \end{pmatrix} & \begin{pmatrix} \mathcal{N}_L \\ \mathcal{E}_L \end{pmatrix} & \begin{pmatrix} \nu_L \\ e_L \end{pmatrix} \\ e_R & \nu_R & \Phi \end{pmatrix}^i, \quad Q_L^i = \left(\begin{pmatrix} d_L & u_L \end{pmatrix} \ D_L \right)^i, \quad Q_R^i = \begin{pmatrix} u_R \\ d_R \\ D_R \end{pmatrix}^i,$$

where the non-chiral quarks, D_L and D_R , are known as Vector-Like-Quarks (VLQs).

The $SU(2)_L$ doublets are in turn given the following names:

$$\begin{aligned} H_d^i &= \begin{pmatrix} H_{d,1} \\ H_{d,2} \end{pmatrix}^i, & E_R^i &= \begin{pmatrix} \mathcal{E}_R \\ \mathcal{N}_R \end{pmatrix}^i, & q_L^i &= \begin{pmatrix} d_L & u_L \end{pmatrix}^i, & \ell_L^i &= \begin{pmatrix} e_L \\ \nu_L \end{pmatrix}^i \\ H_u^i &= \begin{pmatrix} H_{u,1} \\ H_{u,2} \end{pmatrix}^i, & E_L^i &= \begin{pmatrix} \mathcal{N}_L \\ \mathcal{E}_L \end{pmatrix}^i, & \tilde{q}_L^i &= \begin{pmatrix} \tilde{d}_L & \tilde{u}_L \end{pmatrix}^i, & \tilde{\ell}_L^i &= \begin{pmatrix} \tilde{e}_L \\ \tilde{\nu}_L \end{pmatrix}^i, \end{aligned} \quad (4.3)$$

and the name of N^I is unchanged from the UV model.

The charges of the low-scale fields under the remaining symmetry group, eq. (3.14), are calculated by letting the new generators, defined in eq. (3.13), act upon the fields. Consider for instance how \tilde{Q}_L^i is charged under T_T , remembering that it is anti-fundamental under $SU(3)_L$, a singlet under $SU(3)_R$ (seen in tab. 1), and its charge under $U(1)_A$ (seen in tab. 2):

$$(T_T \tilde{Q}_L^i)_l^c = \frac{4}{\sqrt{3}} (T_L^8)_l^l (\tilde{Q}_L^i)_l^c - \frac{5}{3} \underbrace{T_A (\tilde{Q}_L^i)_l^c}_{-\frac{1}{2}(\tilde{Q}_L^i)_l^c} = \frac{1}{3} \delta_l^L (\tilde{Q}_L^i)_L^c - \frac{4}{3} \delta_l^3 (\tilde{Q}_L^i)_3^c + \frac{5}{6} (\tilde{Q}_L^i)_l^c \quad . \quad (4.4)$$

Thus, for $l = 1, 2$ $(\tilde{Q}_L^i)_l^c$ has charge $\frac{3}{2}$ and for $l = 3$ it has $-\frac{1}{2}$. Note that the calculation for $(Q_L^i)_l^c$ is identical, thus it has the same charges. Hence, in terms of the low-scale naming scheme, q_L^i and d_L^i have $U(1)_T$ charges $-\frac{3}{2}$ and $\frac{1}{2}$ respectively, with their scalar counterpart having identical charges. Calculating this for all fields in the theory we arrive at the quantum numbers described in tab. 3.

Table 3: Representations and quantum numbers under the new gauge group, eq. (3.14), for the low-scale fields.

Fields	SU(3) _C	SU(2) _L	U(1) _Y	U(1) _T
H_d^i, E_R^i	1	2	1/2	-3
$H_u^i, E_L^i, \ell_L^i, \tilde{\ell}_L^i$	1	2	-1/2	-2
\tilde{e}_R^i, e_R^i	1	1	1	-1
$\tilde{\nu}_R^i, \tilde{\nu}_R^{i'}, \nu_R^i, \tilde{\Phi}^i, \tilde{\Phi}^{i'}, \Phi^i, \tilde{n}^I, \tilde{n}'^I, N^I, \tilde{s}, \tilde{s}'$	1	1	0	0
\tilde{q}_L^i, q_L^i	3	$\bar{\mathbf{2}}$	1/6	3/2
\tilde{D}_L^i, D_L^i	3	1	-1/3	-1/2
\tilde{u}_R^i, u_R^i	$\bar{\mathbf{3}}$	1	-2/3	3/2
$\tilde{d}_R^i, d_R^i, \tilde{D}_R^i, D_R^i$	3	1	1/3	1/2

Note that e_L^i and e_R^i have opposite hypercharge, this is due to all fields being left-handed Weyl-spinors, hence a Dirac spinor would be constructed by charge conjugating one of the fields, $Q^i = \begin{pmatrix} Q_L^i \\ Q_R^i \end{pmatrix}$, which gives the expected charge structure as in the SM. Keeping this in mind, the hypercharge for the electron becomes negative one as expected. In sec. 6.2 it will also be shown that this field assignment will give the correct electric charges of the corresponding SM fields after the EW symmetry is broken.

4.1 Tree-level masses

Before symmetry breaking the only massive scalars are those that have a quadratic coupling in the UV Lagrangian, seen in sec. 2.2, with mass terms $\mu_1, \mu_2, \mu_3, \mu_4, \eta$. All other scalars and gauge bosons are massless at this energy scale. After spontaneous symmetry breaking, expanding around the VEVs seen in sec. 3, additional quadratic couplings appear in the broken Lagrangian, physically interpreted as particles acquiring mass due to the broken symmetry. Many fields will acquire mass while the SM particles remain massless. The mass terms of scalars are of the form, $\phi\phi^\dagger$, and for fermions $\psi\bar{\psi} = \psi_L\bar{\psi}_R + \psi_R\bar{\psi}_L$, thus the masses can be identified by differentiating the Lagrangian with respect to the fields.

This section describes how the coefficients of the mass terms and mass matrices are found from the Lagrangian, through differentiation. This will be described for scalars, scalars decomposed into CP even and CP odd parts, colored scalars, fermions, and gauge bosons.

4.1.1 Scalars

The mass matrix for scalar fields can be identified as the quadratic terms in the Lagrangian after expanding the fields around the VEVs. The mass matrix for complex scalars, $(M_{(S)}^2)$, is calculated as

$$(M_{(S)}^2)^{ij} = \frac{\partial^2 V}{\partial \phi_i \partial \phi_j^\dagger} \Big|_{\phi_i = \langle \phi_i \rangle} \quad \text{for complex } \phi. \quad (4.5)$$

As described in sec. 4, the fields that are expanded around the VEVs are split into real and imaginary components (CP even and odd). The mass matrices of these components are calculated similarly to eq. (4.5), but differentiating with respect to the unconjugated fields:

$$\frac{1}{2} (M_{(S)}^2)^{ij} = \frac{\partial^2 V}{\partial \phi_i \partial \phi_j} \Big|_{\phi_i = \langle \phi_i \rangle} \quad \text{for real } \phi. \quad (4.6)$$

Note that the reason for expanding the components $(\tilde{L}^i)_2^3$, $(\tilde{L}^i)_2^3$ and $(\tilde{L}^i)_3^3$, into real and imaginary parts in sec. 4 is that these components mix together. Hence blocks 7-11 of the mass matrix, seen in tab. 4, only contain real fields and eq. (4.6) is applicable.

For scalars carrying colored charge, the mass terms can appear as $(\tilde{Q}_L^I)_i^c (\tilde{Q}_{L^I}^*)_c^r$, hence the mass matrix can be calculated from eq. (4.5). However, off-diagonal mass terms, for example $(\tilde{Q}_L^I)_i^c (\tilde{Q}_R^3)_c^r$, also appear in the Lagrangian after symmetry breaking. The mass matrix of these terms is given by

$$(M_{(S)}^2)^{ij} = \frac{\partial^2 V}{\partial \phi_{iL} \partial \phi_{jR}} \Big|_{\phi_i = \langle \phi_i \rangle} \quad \text{for } \phi_L^i = \tilde{Q}_L, \quad \phi_R^i = \tilde{Q}_R. \quad (4.7)$$

All the mass matrices of all scalar fields are calculated and put in a block-diagonal form which can be seen in tab. 4,

Table 4: Blocks of the block-diagonalized scalar mass matrix, the fields and the parameter dependence of each block. The un-colored complex, real, and colored scalars are given in blocks 1-6, 7-11, and 12-18 respectively.

Block #	Basis	UV Parameter Dependence
1	$\{H_d^1\}$	$\{\lambda_{6,9,10}\}$
2	$\{H_d^2, H_d^3\}$	$\{\lambda_{4,6,\dots,10}, \beta_2\}$
3	$\{\tilde{\ell}_L^1\}$	$\{\lambda_{6,7,9,10}\}$
4	$\{\tilde{\ell}_L^2, \tilde{\ell}_L^3, H_u^1\}$	$\{\lambda_{4,6,7,9,10}\}$
5	$\{H_u^2, H_u^3\}$	$\{\lambda_{4,6,\dots,10}, \beta_2\}$
6	$\{\tilde{e}_R^2, \tilde{e}_R^3\}$	$\{\lambda_{4,6}, \beta_2\}$
7	$\{\tilde{\nu}_R^2, \tilde{\nu}_R^3, \tilde{\Phi}^1, \tilde{n}^2\}$	$\{\lambda_{4,\dots,7}, \beta_2\}$
8	$\{\tilde{\nu}_R^1, \tilde{\Phi}^2, \tilde{\Phi}^3, \tilde{n}^1, \tilde{s}\}$	$\{\lambda_{1,\dots,10}, \beta_{1,\dots,5}, \gamma_{4,5,6}, \chi_{1,2,3}\}$
9	$\{\tilde{\nu}_R^{\prime 2}, \tilde{\nu}_R^{\prime 3}, \tilde{\Phi}^{\prime 1}, \tilde{n}^{\prime 2}\}$	$\{\lambda_{4,\dots,7}, \beta_2\}$
10	$\{\tilde{\Phi}^{\prime 2}, \tilde{\Phi}^{\prime 3}, \tilde{n}^{\prime 1}\}$	$\{\lambda_{4,\dots,7}, \beta_2\}$
11	$\{\tilde{s}'\}$	$\{\eta^2, \gamma_{4,5,6}\}$
12	$\{\tilde{q}_L^1\}$	$\{\lambda_{1,2,4,6,9,10}, \alpha_{1,2}\}$
13	$\{\tilde{q}_L^2, \tilde{q}_L^3\}$	$\{\lambda_{1,\dots,10}, \alpha_{1,\dots,6}, \beta_2\}$
14	$\{\tilde{u}_R^1\}$	$\{\lambda_{1,2,4,6,9,10}, \alpha_{1,3,5}\}$
15	$\{\tilde{u}_R^2, \tilde{u}_R^3\}$	$\{\lambda_{1,\dots,10}, \alpha_{1,\dots,6}, \beta_2\}$
16	$\{\tilde{d}_R^1\}$	$\{\lambda_{1,2,4,6,9,10}, \alpha_{1,3,5,7}\}$
17	$\{\tilde{d}_R^2, \tilde{d}_R^3, \tilde{D}_L^2, \tilde{D}_L^3, \tilde{D}_R^1\}$	$\{\lambda_{1,\dots,10}, \alpha_{1,\dots,12}, \beta_{1,2,5}, \gamma_{1,2,3,6}\}$
18	$\{\tilde{D}_L^1, \tilde{D}_R^2, \tilde{D}_R^3\}$	$\{\lambda_{1,\dots,10}, \alpha_{1,\dots,12}, \beta_2, \gamma_{1,3}\}$

where the dagger, \dagger , is used to ensure that fundamental and anti-fundamental field components do not mix.

The scalar fields \tilde{e}_R^1 and $\tilde{\nu}_R^1$ are not appearing in tab. 4 because they remain massless after symmetry breaking, becoming Nambu–Goldstone bosons. Since \tilde{e}_R^1 is complex it carries a total of two Degrees Of Freedom (DOF). Additionally, one eigenvalue of block 6, and two eigenvalues of blocks 7, 9, and 10 are zero. Lastly, one eigenvalue of block 4 is zero, which carries a total of four DOF, due to it being a complex doublet. In total, we find 15 DOF of the massless scalar particles, which give rise to 15 massive gauge bosons, described in the next subsection.

Note that all the scalar mass matrices are symmetric, hence all eigenvalues, m_i^2 , are positive and the mixing matrices that diagonalize all mass matrices by similarity transformations must be hermitian. Furthermore, since all coefficients in the Lagrangian are real, the mixing matrices are also real and hence orthogonal.

4.1.2 Gauge bosons

The Nambu Goldstone’s theorem states that each broken generator gives rise to one massless Nambu-Goldstone boson which is "eaten" by a massless gauge boson, gaining an extra degree of freedom as longitudinal polarization and acquires mass [13]. From sec. 3 15 broken generators were derived, which must give rise to 15 massless Goldstone bosons which in turn give rise to 15 massive bosons. The 15 DOF of the massless scalars was explicitly derived in the previous subsection. The mass matrix of the gauge boson is given by:

$$\frac{1}{2} \left(M_{(G)}^2 \right)_{ab} g^{\mu\nu} = - \left. \frac{\partial^2 \mathcal{L}_{\text{Gauge}}}{\partial G_\mu^a \partial G_\nu^b} \right|_{\phi_i = \langle \phi_i \rangle}. \quad (4.8)$$

All the gauge boson masses and matrices are calculated and shown in tab. 5, and eqs. (4.9), (4.10).

Table 5: Computed masses of the gauge bosons. The first three rows show the squared mass of the given fields, while the last three rows show mass matrices, and which components mix. The mass matrices $M_{G_{R,F}}^2$ and $M_{G_{L,R,F}}^2$ are shown explicitly in eq. (4.9) and (4.10).

Field	Mass Squared
$G_L^{4,5,6,7}$	$\frac{1}{2} (f^2 + p^2 + \omega^2) g_L^2$
$G_R^{1,2}$	$\frac{1}{2} \omega^2 g_R^2$
$G_R^{4,5}$	$\frac{1}{2} (f^2 + p^2) g_R^2$
Basis	Mass Squared Matrix
$\{G_R^6, G_F^1\}$	$M_{G_{R,F}}^2$
$\{G_R^7, G_F^2\}$	$M_{G_{R,F}}^2$
$\{G_L^8, G_R^3, G_R^8, G_F^3\}$	$M_{G_{L,R,F}}^2$

$$M_{G_{R,F}}^2 = \begin{pmatrix} \frac{1}{2}(f^2 + p^2 + \omega^2) g_R^2 & -f\omega g_F g_R \\ -f\omega g_F g_R & \frac{1}{2}(f^2 - \rho^2 + \omega^2) g_F^2 \end{pmatrix} \quad (4.9)$$

$$M_{G_{L,R,F}}^2 = \begin{pmatrix} \frac{2g_L^2}{3}(f^2 + p^2 + \omega^2) & -\frac{\omega^2 g_L g_R}{\sqrt{3}} & \frac{g_L g_R}{3}(-2f^2 - 2p^2 + \omega^2) & \frac{(f^2 - \omega^2) g_F g_L}{\sqrt{3}} \\ -\frac{\omega^2 g_L g_R}{\sqrt{3}} & \frac{1}{2}\omega^2 g_R^2 & -\frac{\omega^2 g_R^2}{2\sqrt{3}} & \frac{1}{2}\omega^2 g_F g_R \\ \frac{g_L g_R}{3}(-2f^2 - 2p^2 + \omega^2) & -\frac{\omega^2 g_R^2}{2\sqrt{3}} & \frac{g_R^2}{6}(4f^2 + 4p^2 + \omega^2) & -\frac{(2f^2 + \omega^2) g_F g_R}{2\sqrt{3}} \\ \frac{(f^2 - \omega^2) g_F g_L}{\sqrt{3}} & \frac{1}{2}\omega^2 g_F g_R & -\frac{(2f^2 + \omega^2) g_F g_R}{2\sqrt{3}} & \frac{g_F^2}{2}(f^2 - \rho^2 + \omega^2) \end{pmatrix} \quad (4.10)$$

The $M_{G_{L,R,F}}^2$ mass matrix has three non-zero eigenvalues, amounting to three massive gauge bosons. The remaining eigenvalue is zero, corresponding to the massless $U(1)_Y$ gauge boson. Hence, 16 gauge boson fields are mixed but only 15 gain mass, as expected.

Similar to the scalars, the mixing matrices that fully diagonalize the gauge boson mass matrices are in general orthogonal transformations.

4.1.3 Fermions

The mass terms for the fermions are $m\psi\bar{\psi}$, which decompose into Weyl-spinors: $m\psi_L\bar{\psi}_R + m\psi_R\bar{\psi}_L$, motivating the following identification of the fermion mass matrix

$$\left(M_{(F)}\right)^{ij} = -\frac{\partial^2 \mathcal{L}_{\text{Fermion}}}{\partial\psi_{L_i}\partial\psi_{R_j}} \Bigg|_{\phi_i=\langle\phi_i\rangle}, \quad (4.11)$$

where $\psi_{L_i} \in Q_L^i$ and $\psi_{R_j} \in Q_R^i$.

The fermion mass matrix is real but not necessarily hermitian, unlike the scalar and gauge boson cases above. To diagonalize the fermion mass matrix the method of Singular-Value-Decomposition (SVD), described in [14], is used. With SVD two orthogonal mixing matrices, L and R , can be found such that $L^T M_{(F)} R = \text{diag}\{m_1, m_2, \dots\}$, where m_i are the fermion masses. The mixed fields are then written as: $\psi'_L = L\psi_L$, and $\psi'_R = R\psi_R$.

The $SU(2)_F$ doublet, N^I , is uncharged under all $U(1)$ groups. Consequently, it is its own antiparticle, known as a Majorana fermion. The mass matrix for a Majorana fermion is calculated as

$$\left(M_{(F)}^2\right)^{ij} = -\frac{\partial^2 \mathcal{L}_{\text{Fermion}}}{\partial\psi_i\partial\psi_j} \Bigg|_{\phi_i=\langle\phi_i\rangle}, \quad \text{for } \psi^i = N^I, \quad (4.12)$$

and is diagonalized by the method of Takagi diagonalization [14], which finds a unitary transformation, Ω , such that $\Omega^T M_{(F)} \Omega = \text{diag}\{m_1, m_2, \dots\}$, where m_i are the Majorana masses.

Leptons do not receive mass at tree level, as in eq. (2.11) they only interact with the colored scalars, \tilde{Q}_L and \tilde{Q}_R , which do not receive any VEV, resulting in the leptons not developing mass through any Higgs mechanism.

Using eq. (4.11), it is found that the up type quarks $u^i = \begin{pmatrix} u_L \\ u_R^c \end{pmatrix}^i$ remain massless.

The mass matrix for the down type quarks, d^i , and vector-like quarks, D^i becomes:

$$M_{\text{down}} = \frac{1}{\sqrt{2}} \begin{pmatrix} 0 & 0 & 0 & 0 & 0 & 0 \\ 0 & 0 & 0 & 0 & 0 & 0 \\ 0 & 0 & 0 & 0 & 0 & 0 \\ 0 & 0 & 0 & 0 & py_3 & -fy_1 \\ 0 & 0 & \omega y_1 & -py_3 & 0 & 0 \\ 0 & \omega y_2 & 0 & -fy_2 & 0 & 0 \end{pmatrix}, \quad (4.13)$$

written in the basis $\begin{pmatrix} d_L^i \\ D_L^i \end{pmatrix} M_{\text{down}} \begin{pmatrix} d_R^i & D_R^i \end{pmatrix}$.

Using SVD M_{down} is diagonalized, resulting in three massless down-type quarks, and three massive VLQs. M_{down} can be divided into the 3×3 blocks:

$$M_D^{\text{mix}} = \frac{1}{\sqrt{2}} \begin{pmatrix} 0 & 0 & 0 \\ 0 & 0 & \omega y_1 \\ 0 & \omega & 0 \end{pmatrix}, \quad M_D^{\text{diag.}} = \frac{1}{\sqrt{2}} \begin{pmatrix} 0 & py_3 & -fy_1 \\ -py_3 & 0 & 0 \\ -fy_2 & 0 & 0 \end{pmatrix}, \quad (4.14)$$

where M_D^{mix} can be identified as the mixing matrix between D_L^i and d_R^i , and $M_D^{\text{diag.}}$ is the mass matrix for D_L, D_R .

Rotating the fields into a diagonal form results in the fields: $\mathfrak{d}_L^i, \mathfrak{d}_R^i, \mathfrak{D}_L^i$, and \mathfrak{D}_R^i , related to the original fields by:

$$\begin{pmatrix} \mathfrak{d}_L^i \\ \mathfrak{D}_L^i \end{pmatrix} = L \begin{pmatrix} d_L^i \\ D_L^i \end{pmatrix}, \quad \begin{pmatrix} \mathfrak{d}_R^i \\ \mathfrak{D}_R^i \end{pmatrix} = R \begin{pmatrix} d_R^i \\ D_R^i \end{pmatrix}, \quad (4.15)$$

where \mathfrak{d}_L^i and \mathfrak{d}_R^i become massless, corresponding to the SM down type quarks, while \mathfrak{D}_L^i and \mathfrak{D}_R^i become massive VLQs.

For N^I , using eq. (4.12), the mass matrix becomes

$$M_N = \begin{pmatrix} 0 & 2\sqrt{2}wy_4 \\ 2\sqrt{2}wy_4 & 0 \end{pmatrix}, \quad (4.16)$$

which after using Takagi diagonalization gives degenerate masses of N^1 and N^2 :

$$m_N = 2\sqrt{2}wy_4. \quad (4.17)$$

5 Effective Field Theory

The construction of an EFT is a general mathematical procedure to simplify problems by approximating away irrelevant information of a certain problem. For instance, we do not need Newton's law of gravity to describe dynamics on the surface of Earth [9].

In the context of Quantum Field Theory, one integrates out heavy fields of the theory. The theory containing the remaining fields is known as an EFT. At low energies, these heavy states cannot be produced as initial or final states of any Feynman diagram, but can only appear as virtual particles in loops. Although not directly detectable, these particles still modify observable quantities. Calculating how the observed parameters in the EFT are modified by the full theory, with heavy particles, is done by EFT matching. This matching procedure calculates effective couplings of a model only containing light particles, matched to the full, high-energy theory, but considered at low energies such that the heavy particles only appear in loops.

This section details the EFT Lagrangian, the fields it contains, and couplings. Moreover, a formal description of the construction of the EFT is given, as well as the matching conditions and mathematical tools needed to calculate loop integrals.

5.1 EFT fields and Lagrangian

To construct an EFT, firstly, the light and heavy fields must be identified. Consequently, all fields must be written in the mass basis, by diagonalizing the mass matrices in sec. 4.1. To motivate the following choice of light and heavy fields, a scan of the mass spectrum is performed in sec. 7.

The light scalar fields that are chosen to be kept light, and enter the EFT, are: $\tilde{q}_L^1, \tilde{d}_R^1$, and the down-type Higgs-doublet, H_d^1 . The fields are relabeled in the EFT as: $\tilde{q}_L^1 \equiv \mathcal{R}$, $\tilde{d}_R^1 \equiv \mathcal{S}$, and $H_d^1 \equiv \mathcal{H}$, where colored scalars are also known as scalar Lepto-Quarks (LQs). The scalar masses are described in sec. 4.1. Diagonalizing the fermion masses, using SVD, results in three massless fermions, \mathfrak{d}_L^i and \mathfrak{d}_R^i , corresponding to the three generations of left and right handed down-quarks in the SM; and six massive VLQ components, \mathfrak{D}_L^i and \mathfrak{D}_R^i . The massless fermions are kept in the EFT, while only the first generation of the massive VLQ, \mathfrak{D}_L^1 and \mathfrak{D}_R^1 , are put in the EFT. The \mathfrak{d}_L^i particles are put into $\mathfrak{q}_L^i = \begin{pmatrix} \mathfrak{d}_L^i & u_L^i \end{pmatrix}$.

All other fermions and leptons are massless and kept in the EFT, except for the $SU(2)_F$ doublet N^I . For the gauge bosons, only the broken generators will have a mass which is of the scale of the VEVs and thus will be integrated out. The field content of the EFT is summarized in tab. 6.

Table 6: All scalars, fermions and gauge bosons in the EFT, their representations and charges as calculated in sec. 3.2.

	SU(3) _C	SU(2) _L	U(1) _Y	U(1) _B
Scalars				
\mathcal{H}	1	2	1/2	0
\mathcal{R}	3	$\bar{2}$	1/6	1/3
\mathcal{S}	$\bar{3}$	1	1/3	-1/3
Fermions				
E_R^i	1	2	1/2	0
E_L^i	1	2	-1/2	0
ℓ_L^i	1	2	-1/2	0
e_R^i	1	1	1	0
ν_R^i	1	1	0	0
Φ^i	1	1	0	0
q_L^i	3	$\bar{2}$	1/6	1/3
\mathcal{D}_L^1	3	1	-1/3	1/3
u_R^i	$\bar{3}$	1	-2/3	-1/3
\mathcal{D}_R^i	$\bar{3}$	1	1/3	-1/3
\mathcal{D}_R^1	3	1	1/3	-1/3
Gauge Bosons				
G_C	8	1	0	0
G_L	1	3	0	0
G_Y	1	1	0	0

The most general (dimension four) Lagrangian containing all these fields has a scalar potential given by eq. (5.1), and fermion interactions given by eq. (5.2). That no other combinations are possible was confirmed using SARAH [15].

$$\begin{aligned} \mathcal{L}_{\text{Scalar}}^{\text{EFT}} = & m_{\mathcal{H}}^2 |\mathcal{H}|^2 + m_{\mathcal{R}}^2 |\mathcal{R}|^2 + m_{\mathcal{S}}^2 |\mathcal{S}|^2 + Z_1 |\mathcal{H}|^4 + Z_2 |R|^4 + Z_3 |S|^4 + Z_4 |\mathcal{H}|^2 |\mathcal{R}|^2 \\ & + Z_5 |\mathcal{R}|^2 |\mathcal{S}|^2 + Z_6 |\mathcal{H}|^2 |\mathcal{S}|^2 + Z_7 (\mathcal{R}\mathcal{H})(\mathcal{H}^\dagger \mathcal{R}^\dagger) + A(\mathcal{H}^\dagger \mathcal{R} \mathcal{S} + \mathcal{H} \mathcal{R}^\dagger \mathcal{S}^\dagger) \end{aligned} \quad (5.1)$$

$$\begin{aligned} \mathcal{L}_{\text{Fermions}}^{\text{EFT}} = & M_E^{ij} E_L^i E_R^j + M_{\ell E}^{ij} \ell_L^i E_R^j + M_{\mathcal{D}}^{ij} \mathcal{D}_L^1 \mathcal{D}_R^1 + M_{\mathcal{D}}^{\prime ij} \mathcal{D}_L^1 \mathcal{D}_R^i + M_{\nu}^{ij} \nu_R^i \nu_R^j \\ & + M_{\Phi}^{ij} \Phi^i \Phi^j + M_{\nu \Phi}^{ij} \nu_R^i \Phi^j + Y_u^{ij} \mathcal{H} q_L^i u_R^j + Y_d^{ij} \mathcal{H}^\dagger q_L^i \mathcal{D}_R^j + Y_{\mathcal{D}}^{ij} \mathcal{H}^\dagger q_L^i \mathcal{D}_R^1 \\ & + Y_{\nu 1}^{ij} \mathcal{H} \ell_L^i \nu_R^j + Y_{\nu 2}^{ij} \mathcal{H} E_L^i \nu_R^j + Y_{\nu 3}^{ij} \mathcal{H}^\dagger E_R^i \nu_R^j + Y_{e 1}^{ij} \mathcal{H}^\dagger \ell_L^i e_R^j + Y_{e 2}^{ij} \mathcal{H}^\dagger E_L^i e_R^j \\ & + Y_{\Phi 1}^{ij} \mathcal{H} \ell_L^i \Phi^j + Y_{\Phi 2}^{ij} \mathcal{H} E_L^i \Phi^j + Y_{\Phi 3}^{ij} \mathcal{H}^\dagger E_R^i \Phi^j + \Omega_1^{ij} \mathcal{R} \ell_L^i \mathcal{D}_R^j + \Omega_2^{ij} \mathcal{R} E_L^i \mathcal{D}_R^j \\ & + \Omega_3 \mathcal{R} \ell_L^i \mathcal{D}_R^1 + \Omega_4 \mathcal{R} E_L^i \mathcal{D}_R^1 + \Omega_5^{ij} \mathcal{R} E_R^i u_R^j + \Omega_6^{ij} \mathcal{R}^\dagger q_L^i \nu_R^j + \Omega_7^{ij} \mathcal{R}^\dagger q_L^i \Phi^j \\ & + \Omega_8 \mathcal{R}^\dagger E_R^i \mathcal{D}_L^1 + \Theta_1^{ij} \mathcal{S} \ell_L^i q_L^j + \Theta_2^{ij} \mathcal{S} E_L^i q_L^j + \Theta_3^i \mathcal{S} \nu_R^i \mathcal{D}_L^1 + \Theta_4^i \mathcal{S} \Phi^i \mathcal{D}_L^1 \\ & + \Theta_5^{ij} \mathcal{S}^\dagger e_R^i u_R^j + \Theta_6^{ij} \mathcal{S}^\dagger \nu_R^i \mathcal{D}_R^j + \Theta_7^{ij} \mathcal{S}^\dagger \Phi^i \mathcal{D}_R^j + \Theta_8^i \mathcal{S}^\dagger \nu_R^i \mathcal{D}_R^1 + \Theta_9^i \mathcal{S}^\dagger \Phi^i \mathcal{D}_R^1 \\ & + \text{h.c} \end{aligned} \quad (5.2)$$

Note that for instance the term $Y_d^{ij} \mathcal{H}^\dagger q_L^i d_R^j$ contracts two anti-fundamental SU(2)_L doublets implicitly through the Levi-Civita tensor. This structure does not appear in the UV

Lagrangian, eq. (2.11), and is consequently zero at tree level. The global symmetry $U(1)_T$ does not appear in the SM, hence we break it softly, and it does not appear in tab. 6.

Altogether, we have 4 mass terms m_i^2 , 6 mass matrices M_i , 7 quartic couplings Z_i , one trilinear coupling A , and 28 Yukawa couplings, Y_i, Ω_i, Θ_i . Note that after diagonalizing the fermion masses, the mass matrix $M'_2 = 0$ at tree level, but can in general become nonzero from higher order corrections.

The gauge Lagrangian is identical to that of eq. (2.12), but instead containing the scalars and fermions in the EFT, tab. 6. The coupling constants g_C , and g_L remain the same for the EFT, since the $SU(3)_C$ is not broken, and the fact that the light $SU(2)_L$ gauge bosons, $G_L^{1,2,3}$, do not mix with any other bosons. The hypercharge coupling, g_Y , appears in the EFT Lagrangian as:

$$\mathcal{D}_\mu \supset g_Y T_Y^a G_{Y\mu}^a, \quad (5.3)$$

where T_Y^a is defined in eq. (3.13), and $G_{Y\mu}^a$ is identified as the massless eigenvector of $M_{G_{L,R,F}}^2$ seen in eq. (4.10), giving

$$G_Y^a = \frac{1}{\sqrt{4g_L^2 + g_R^2}} (g_R G_L^8 + \sqrt{3} g_L G_R^3 + g_L G_R^8), \quad (5.4)$$

The vector bosons G_L^8, G_R^3 , and G_R^8 all mix to G_Y and tree massive vector bosons. Finding the orthogonal mixing matrix and rotating the gauge Lagrangian in eq. (2.12) to the broken mass basis, g_Y can be identified as the term in front of $T_Y G_{Y\mu}^a$, as in eq. (5.3). A more detailed derivation is found in [10]. It is thus found that

$$g_Y = \frac{\sqrt{3} g_L g_R}{\sqrt{4g_L^2 + g_R^2}}. \quad (5.5)$$

5.2 Formalism of EFTs

Considering a Lagrangian containing particles with a wide mass-spectrum, the Lagrangian can be divided into light fields, $\{\phi^L\}$, and heavy fields, $\{\phi^H\}$, such that $\mathcal{L}_{UV}(\{\phi^L\}, \{\phi^H\}) = \mathcal{L}_{\text{Light}}(\{\phi^L\}) + \mathcal{L}_{\text{Mix}}(\{\phi^L\}, \{\phi^H\}) + \mathcal{L}_{\text{Heavy}}(\{\phi^H\})$. The decoupling theorem states that the massive fields will not impact the dynamics of the particles at lower energies [16], which motivates the construction of the EFT. The EFT is constructed by integrating out all heavy fields such that $\mathcal{L}_{\text{EFT}} \equiv \mathcal{L}_{\text{Light}}$.

The matching between the original UV theory and the EFT is done by matching the scattering matrix elements between the theories at a low energy scale, which can be done by matching the one-light-particle-irreducible amplitudes (1PI) [17] [18].

$$\mathcal{M}_{\text{EFT}}(\{\phi^L\}) \equiv \mathcal{M}_{\text{UV}}(\{\phi^L\}, \{\phi^H\})_{p^2 \leq M^2}, \quad (5.6)$$

where $p^2 \leq M^2$ indicates that the matching takes place at energies lower or equal to the heaviest $\{\phi^H\}$ field with mass M .

Following the structure of [18], these scattering matrices can be split into tree-level, loop-level and counter-term parts

$$\mathcal{M}_{\text{EFT}}^{\text{tree}} + \mathcal{M}_{\text{EFT}}^{\text{loop}} + \mathcal{M}_{\text{EFT}}^{\text{ct}} = \mathcal{M}_{\text{UV}}^{\text{tree}} + \mathcal{M}_{\text{UV}}^{\text{loop}} + \mathcal{M}_{\text{UV}}^{\text{ct}},$$

which can be rewritten as:

$$\mathcal{M}_{\text{EFT}}^{\text{tree}} = -\mathcal{M}_{\text{EFT}}^{\text{loop}} - \mathcal{M}_{\text{EFT}}^{\text{ct}} + \mathcal{M}_{\text{UV}}^{\text{tree}} + \mathcal{M}_{\text{UV}}^{\text{loop}} + \mathcal{M}_{\text{UV}}^{\text{ct}}. \quad (5.7)$$

Effectively, we take the finite part of eq. (5.7) to be the matching condition, as the divergences of individual terms in the above expression can be neglected as they will cancel. In the UV limit, the light particles will not affect the amplitudes, and the UV-divergences are canceled by the UV counter-terms. Furthermore, the IR divergences are also canceled by the construction of the EFT to match the UV theory in the IR limit [19].

The loop integrals can be expanded in $\mathcal{M}_{\text{loop}}^{\text{UV}}$ and $\mathcal{M}_{\text{loop}}^{\text{EFT}}$ where the loop integral of the EFT part become scaleless and vanish in dimensional regularization [18]

$$\mathcal{M}_{\text{tree}}^{\text{EFT}} = \mathcal{M}_{\text{tree}}^{\text{UV}} + \mathcal{M}_{\text{loop,expanded}}^{\text{UV}} + (\mathcal{M}_{\text{ct}}^{\text{UV}} - \mathcal{M}_{\text{ct}}^{\text{EFT}}). \quad (5.8)$$

A more complete treatment of the theory of EFT is described in [19].

5.3 EFT matching equations

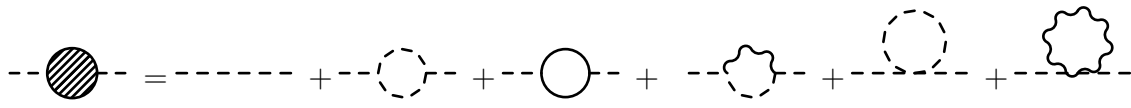
To match the EFT to the high scale theory, all couplings in eq. (5.1) and (5.2), must be matched. That is, corrections for all masses, trilinear scalar couplings, Yukawa couplings, gauge couplings, and quartic couplings must be calculated. For simplicity, loops with only heavy particles are considered. That is, external legs can only be light particles, and no loops with mixed light and heavy particles appear. The different topologies contributing to the one loop matching can be seen in the following eqs. (5.10), (5.11), (5.12), (5.13), and (5.14).

The corrected mass can be identified by first calculating the propagator correction, calculated as the sum of all 1PI diagram with two external legs. The physical mass can then be recognized by first writing the two-point correlation function, using the corrected propagator, as a geometric series and identifying the physical mass as its pole [13]. We then arrive at:

$$m_{\text{EFT}} = m_0 + \delta m \quad (5.9)$$

where δm is the corrected propagator and m_0 is the tree level mass using the Modified Minimal Subtraction scheme ($\overline{\text{MS}}$) described in more detail in the next subsection.

Written diagrammatically, the mass term for the scalars becomes:



$$-\text{---} \text{---} \text{---} \text{---} = \text{---} \text{---} \text{---} \text{---} + \text{---} \text{---} \text{---} \text{---} + \text{---} \text{---} \text{---} \text{---} + \text{---} \text{---} \text{---} \text{---} + \text{---} \text{---} \text{---} \text{---} + \text{---} \text{---} \text{---} \text{---} \quad (5.10)$$

where the first term is the tree level mass, and the other diagrams constitute the mass correction, δm .

The fermions mass term is:

$$\text{---} \text{---} \text{---} \text{---} \text{---} \text{---} = \text{---} \text{---} \text{---} \text{---} \text{---} \text{---} + \text{---} \text{---} \text{---} \text{---} \text{---} \text{---} + \text{---} \text{---} \text{---} \text{---} \text{---} \text{---} \quad (5.11)$$

The effective trilinear couplings are simply calculated as the sum of the tree level contribution plus the higher order corrections. The effective Yukawa coupling is:

$$\begin{aligned} \text{---} \text{---} \text{---} \text{---} \text{---} \text{---} &= \text{---} \text{---} \text{---} \text{---} \text{---} \text{---} + \text{---} \text{---} \text{---} \text{---} \text{---} \text{---} + \text{---} \text{---} \text{---} \text{---} \text{---} \text{---} + \text{---} \text{---} \text{---} \text{---} \text{---} \text{---} \\ &+ \text{---} \text{---} \text{---} \text{---} \text{---} \text{---} + \text{---} \text{---} \text{---} \text{---} \text{---} \text{---} + \text{---} \text{---} \text{---} \text{---} \text{---} \text{---} \end{aligned} \quad (5.12)$$

The effective scalar trilinear is:

$$\text{---} \text{---} \text{---} \text{---} \text{---} \text{---} = \text{---} \text{---} \text{---} \text{---} \text{---} \text{---} + \text{---} \text{---} \text{---} \text{---} \text{---} \text{---} + \text{---} \text{---} \text{---} \text{---} \text{---} \text{---} + 3 \text{---} \text{---} \text{---} \text{---} \text{---} \text{---} + \text{---} \text{---} \text{---} \text{---} \text{---} \text{---} \quad (5.13)$$

where the last two diagrams of eq. (5.12), and the last term in eq. (5.13), are the external leg corrections at one loop level, comprising the wavefunction renormalization. They consist of the 1PI diagrams with one loop and are given by the corrections to the mass terms in eq. (5.10) and (5.11).

The quartic scalar interactions are approximated by the tree level matching conditions, which still allows for dependence on the heavy fields,

$$\begin{aligned} \text{---} \text{---} \text{---} \text{---} \text{---} \text{---} &= \text{---} \text{---} \text{---} \text{---} \text{---} \text{---} + \text{---} \text{---} \text{---} \text{---} \text{---} \text{---} + \text{---} \text{---} \text{---} \text{---} \text{---} \text{---} + \text{---} \text{---} \text{---} \text{---} \text{---} \text{---} \\ &+ \text{---} \text{---} \text{---} \text{---} \text{---} \text{---} + \text{---} \text{---} \text{---} \text{---} \text{---} \text{---} + \text{---} \text{---} \text{---} \text{---} \text{---} \text{---} \end{aligned} \quad (5.14)$$

Note that in the limit of zero external momentum the last three diagrams involving the vector boson will tend to zero, as there is no momentum that is integrated over.

The mass term for the gauge bosons calculated at one loop is calculated similarly to eq. (5.10) and (5.11), but with two external gauge bosons. The effective gauge coupling can be calculated by considering the one loop corrections to Feynman diagrams with one external gauge boson and either two external fermions or two scalars. However, this work considers the gauge boson effective masses and effective gauge couplings at tree level.

The above diagrams require the Feynman rules of the UV theory to be known. Due to the complexity of the scalar potential, a general method of identifying the possible vertex

interactions is needed. This can be calculated by differentiating the Lagrangian, expanded around the VEVs, with respect to the different fields. The trilinear and quartic scalar vertex factors, $T_{ijk}^{(S)}$ and $Q_{ijkl}^{(S)}$ are then given by:

$$T_{ijk}^{(S)} = \frac{1}{S} \left. \frac{\partial^3 V}{\partial \phi^i \partial \phi^j \partial \phi^k} \right|_0, \quad Q_{ijkl}^{(S)} = \frac{1}{S} \frac{\partial^4 V}{\partial \phi^i \partial \phi^j \partial \phi^k \partial \phi^l}, \quad (5.15)$$

where i, j, k, l are the index component of a list of all scalars, $\phi^i = \{H_d^1, H_d^{1\dagger}, \tilde{e}_R^1, \tilde{e}_R^{1\dagger}, \dots\}^i$, the evaluation at zero for the trilinear term ensures any remaining fields after differentiation are set to zero, and S is a symmetry factor, for instance, for four identical field $S = 4!$.

Similarly, the Yukawa interactions, $T_{ijk}^{(F)}$, can be identified by differentiating the fermion Lagrangian with respect to two fermion fields and one scalar field. Thus we can write:

$$\begin{array}{ccc} \begin{array}{c} \phi_j \\ \diagdown \\ \phi_i \end{array} \text{---} \phi_k = -iT_{ijk}^{(S)}, & \begin{array}{c} \phi_j \\ \diagdown \\ \phi_i \end{array} \times \begin{array}{c} \phi_l \\ \diagup \\ \phi_k \end{array} = -iQ_{ijkl}^{(S)}, & \begin{array}{c} \psi_j \\ \diagdown \\ \psi_i \end{array} \text{---} \phi_k = -iT_{ijk}^{(F)}, \end{array} \quad (5.16)$$

where the factor $-i$ is necessary to be consistent with the propagator and gauge sector Feynman rules.

The gauge Lagrangian, eq. 2.12, is identical to that of the SM, but with additional SU(3) gauge symmetries, additional fermions, and charged scalars. The trilinear and quartic couplings involving SU(3) vector bosons are well known and described in [20, 21], while in principle they could be derived in a similar manner as for the scalars and fermions. The relevant Feynman rules are:

$$\begin{array}{ccc} \begin{array}{c} \psi_j \\ \diagdown \\ \psi_i \end{array} \text{---} G_X^{a\mu} = ig_X \gamma^\mu (T_X^a)_j^i \equiv i\gamma^\mu T_{ija}^{(GF)}, & \begin{array}{c} \phi_j \\ \diagdown \\ \phi_i \end{array} \text{---} G_X^{a\mu} = ig_X (-p_1^\mu + p_2^\mu) (T_X^a)_j^i \equiv i(p_1^\mu + p_2^\mu) T_{ija}^{(GS)}, \\ \begin{array}{c} \phi_j \\ \diagdown \\ \phi_i \end{array} \text{---} \begin{array}{c} G_X^{a\mu} \\ G_X^{b\mu} \end{array} = ig_X^2 (T_X^a)_j^i (T_X^b)_j^i \equiv iT_{ijab}^{(GSS)}, \end{array} \quad (5.17)$$

where $G_X^{a\mu}$ is a list of all heavy vector bosons of type $X = L, R, F$. Note that the fermions in $T_{ija}^{(GF)}$ are already rotated to the mass basis, while the scalars and gauge bosons are not. There is not any two vector boson to scalar vertex contributing due to the outgoing scalar always being of the scale of the VEVs, thus heavy.

The propagators for the scalars, fermions and vector bosons with momentum k are:

$$\begin{array}{ccc} \text{---} \times \text{---} = \frac{i}{k^2 - m^2}, & \text{---} \times \text{---} = \frac{i(\not{k} + m)}{k^2 - m^2}, & \text{---} \times \text{---} = -i \frac{g_{\mu\nu} - k_\mu k_\nu / m^2}{k^2 - m^2}. \end{array} \quad (5.18)$$

The scalar propagator mixes the scalar and its complex component, and the fermion Dirac propagator interchanges the chirality of fermions, hence the scalars and Weyl spinors are mixed in the propagators above.

In eq. 5.15 the Lagrangian is differentiated with respect to the UV fields, however, the interactions take place in the mass basis. Consequently, the tensors $T_{ijk}^{(S)}$, $Q_{ijkl}^{(S)}$, $T_{ijk}^{(F)}$, $T_{ija}^{(GS)}$ and $T_{ija}^{(GF)}$, need to be rotated into the mass basis. For instance, the trilinear terms of the scalars appear as:

$$\mathcal{L}_{\text{mass-basis}} \supset T'_{abc}{}^{(S)} \phi'^a \phi'^b \phi'^c = T_{ijk}^{(S)} (O_\phi)_{ai} (O_\phi)_{bj} (O_\phi)_{ck} \phi^a \phi^b \phi^c \quad , \quad (5.19)$$

where the primed fields and tensors denote fields being in the mass basis, and (O_ϕ) denotes the rotation matrix for the scalars. Hence the trilinear term in the mass basis is:

$$T'_{abc}{}^{(S)} = T_{ijk}^{(S)} (O_\phi)_{ai} (O_\phi)_{bj} (O_\phi)_{ck} \quad , \quad (5.20)$$

and equivalently for the four-point vertex,

$$Q'_{abcd}{}^{(S)} = T_{ijkl}^{(S)} (O_\phi)_{ai} (O_\phi)_{bj} (O_\phi)_{ck} (O_\phi)_{dl} \quad . \quad (5.21)$$

For the Yukawa interactions, the scalar field will still be in the gauge-basis, and must be rotated:

$$T_{ijk}^{(F)} = T'_{ajk}{}^{(F)} (O_\phi)_{ai} \quad . \quad (5.22)$$

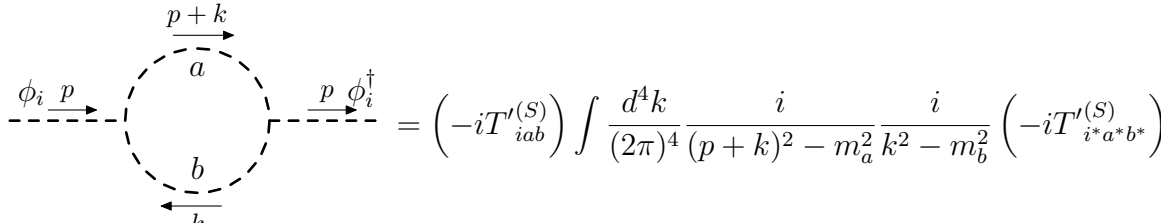
The trilinear couplings involving the vector boson are rotated by the gauge mixing matrix, (O_G) , and considering the gauge-fermion and gauge-scalar interactions, we get:

$$\begin{aligned} T'_{abc}{}^{(GF)} &= T_{ijk}^{(GF)} (O_G)_{ck}, & T'_{abc}{}^{(GS)} &= T_{ijk}^{(GS)} (O_\phi)_{ai} (O_\phi)_{bj} (O_G)_{ck}, \\ T'_{abcd}{}^{(GSS)} &= T_{ijkl}^{(GSS)} (O_\phi)_{ai} (O_\phi)_{bj} (O_G)_{ck} (O_G)_{dl} \quad . \end{aligned} \quad (5.23)$$

Due to the complexity of the mass matrices, derived in sec. 4.1, it is not feasible to analytically rotate the fields into the mass basis. Hence a numerical approach is needed and will be described in sec. 7.

5.4 Loop integrals

Considering the second term in eq. (5.10), with some initial and final particle, i , with momentum, p , and the particles a and b in the loop with momentum $p+k$ and k respectively,



$$= \left(-i T'_{iab}{}^{(S)} \right) \int \frac{d^4 k}{(2\pi)^4} \frac{i}{(p+k)^2 - m_a^2} \frac{i}{k^2 - m_b^2} \left(-i T'_{i^* a^* b^*}{}^{(S)} \right) \quad (5.24)$$

ignoring the $i\epsilon$ prescription, and the complex conjugated indices denotes the index of corresponding complex conjugated field, required due to the propagator in eq. (5.18).

The loop integral can be calculated using dimensional regularization, for simplicity consider $m_a = m_b$ so $b = a$, in the zero external momentum limit, $p \rightarrow 0$, the integral, I , becomes

$$I = \int \frac{d^4k}{(2\pi)^4} \frac{1}{(k^2 - m_a^2)^2} \quad . \quad (5.25)$$

Dimensional regularization is an analytic continuation of the number of space-time dimensions, made by the following replacement: $\int \frac{d^4k}{(2\pi)^4} \rightarrow \int \mu^{4-d} \frac{d^d k}{(2\pi)^d}$, where μ is a dimensional constant to keep the correct units, and d the dimension parameter which in the end is taken to approach 4 [22]. The motivation of dimensional regularization is to decrease the power of d^4k to ensure that the integral converges. We also define ϵ such that $d = 4 - \epsilon$, so $\epsilon \rightarrow 0$ as $d \rightarrow 4$. The integral in dimensional regularization, I_d , then becomes

$$I_d = \int \mu^\epsilon \frac{d^d k}{(2\pi)^d} \frac{1}{(k^2 - m_a^2)^2} \quad . \quad (5.26)$$

which can be seen to converge for $d < 4$.

Rewriting this in terms of spherical coordinates, see [13, 22], I_d becomes

$$I_d = \mu^\epsilon \int \frac{d\Omega_d}{(2\pi)^d} \int_0^\infty dp \frac{p^{d-1}}{(p^2 - m_a^2)^2} \quad , \quad (5.27)$$

where the first integral is the volume of a d -dimensional sphere, $\int d\Omega_d = 2\pi^{\frac{d}{2}}/\Gamma(\frac{d}{2})$. The second integral can be solved using a change of variables and the Euler beta function,

$$\int_0^\infty dp \frac{p^{d-1}}{(p^2 - m_a^2)^2} = \frac{1}{2} \left(\frac{1}{m_a^2} \right)^{2-\frac{d}{2}} \frac{\Gamma\left(2 - \frac{d}{2}\right) \Gamma\left(\frac{d}{2}\right)}{\Gamma(2)} \quad ,$$

I_d then becomes

$$I_d = \frac{\mu^\epsilon}{(4\pi)^d} \Gamma\left(2 - \frac{d}{2}\right) \left(\frac{1}{m_a^2}\right)^{2-\frac{d}{2}} = \frac{\mu^\epsilon}{(4\pi)^2} (4\pi)^{\epsilon/2} \Gamma\left(\frac{\epsilon}{2}\right) m_a^{-\epsilon} \quad . \quad (5.28)$$

Laurent expanding in ϵ ,

$$\Gamma\left(\frac{\epsilon}{2}\right) = \frac{2}{\epsilon} - \underbrace{\Gamma'(1)}_{\equiv \gamma_E} + \mathcal{O}(\epsilon) \quad ,$$

$$\left(\frac{m^2}{4\pi\mu^2}\right)^{-\epsilon/2} = \exp\left(-\frac{\epsilon}{2} \ln\left(\frac{m^2}{4\pi\mu}\right)\right) = 1 - \frac{\epsilon}{2} \ln\left(\frac{m^2}{4\pi\mu^2}\right) + \mathcal{O}(\epsilon^2) \quad ,$$

where γ_E is Euler's constant, we get

$$I_d = \frac{1}{(4\pi)^2} \left(\frac{2}{\epsilon} - \gamma_E - \ln\left(\frac{m_a^2}{\mu^2}\right) - \ln(4\pi) + \mathcal{O}(\epsilon) \right) \quad . \quad (5.29)$$

The final integral still diverges as $\epsilon \rightarrow 0$, these divergences will in general be canceled by counter terms [23]. Using the Minimal Subtraction (MS) renormalization scheme, the $1/\epsilon$ pole is absorbed into the counterterm and subtracted away. Furthermore, in the $\overline{\text{MS}}$ -scheme, one takes $\mu^2 \rightarrow \mu^2 \frac{e^{\gamma_E}}{4\pi}$, such that the other finite constants in I_d are canceled. Thus, the poles are subtracted, leaving the finite functional dependence unaffected.

$$I_d^{\overline{\text{MS}}} = \frac{1}{(4\pi)^2} \left(-\ln \left(\frac{m_a^2}{\mu^2} \right) + \mathcal{O}(\epsilon) \right) . \quad (5.30)$$

We are now free to take the limit $d \rightarrow 4$, eq. (5.24) becomes for $a = b$ and $p \rightarrow 0$:

$$T'_{iaa}{}^{(S)} T'^{(S)}_{i^*a^*a^*} \frac{1}{16\pi^2} \ln \left(\frac{\mu^2}{m_a^2} \right) . \quad (5.31)$$

Noteworthy is that the final expression depends on μ , which is the renormalization scale. In general, the renormalization scale will never appear in observables [22]. As the matching is performed at the breaking scale of the smallest VEV in eq. (3.1), μ is taken to be this scale.

In general, a loop integral with N propagators, with masses m_0, \dots, m_{N-1} , and P fermions, with four-momentum of the i th fermion being p_{μ_i} , becomes:

$$I_{\mu_1 \dots \mu_P}^N(p_1, \dots, p_{N-1}; m_0, \dots, m_{N-1}) = \frac{(2\pi\mu)^{4-d}}{i\pi^2} \int d^d k \frac{k_{\mu_1} \dots k_{\mu_P}}{(k^2 - m_0^2)((p_1 + k)^2 - m_1^2) \dots ((p_{N-1} + k)^2 - m_{N-1}^2)} . \quad (5.32)$$

This integral can generally be solved using the Passarino-Veltman functions [24]. It can be shown that this tensor can be reduced, through differentiation, to linear combinations of scalar integrals. The Passarino-Veltman functions are usually denoted by the N th character of the alphabet, $I_{\mu_1 \dots \mu_P}^1 = A_{\mu_1 \dots \mu_P}$, $I_{\mu_1 \dots \mu_P}^2 = B_{\mu_1 \dots \mu_P}$, and so on. The calculated loop integral in eq. (5.24) is hence denoted by $iB_0(p = 0; m_a, m_b = m_a)$, where the subscript zero denotes the scalar integrals. This tensor reduction can be done systematically and is hence implemented in several computer packages, to reduce lengthy expressions [25]. One such program, to calculate these loop integrals is Package X [26] for Mathematica used in this thesis.

In total, summing over all heavy particles in the loop, the second term in eq. (5.24) becomes

$$\begin{array}{c} \phi_i \\ \text{---} \end{array} \begin{array}{c} a \\ \text{---} \end{array} \begin{array}{c} \phi_i^\dagger \\ \text{---} \end{array} \begin{array}{c} b \\ \text{---} \end{array} = \frac{1}{2!} \sum_{a,b \in \{\phi^H\}} T'_{iab}{}^{(S)} T'^{(S)}_{i^*a^*b^*} iB_0(0; m_a, m_b) , \quad (5.33)$$

where $\{\phi^H\}$ is a list of all heavy scalar fields, and the prefactor $\frac{1}{2!}$ is needed to avoid double counting. The other terms are calculated similarly and additional examples are found in Appendix B.

6 Matching to the Standard Model

All calculations throughout this thesis have taken place at the energy scale of the VEVs, described in sec. 3. Due to the couplings and masses being energy dependent, we must run the parameters down to SM-energies to compare these with observables. Specifically, this is achieved by studying the RG evolution and β -functions, which is used to run to the Electroweak Symmetry-Breaking (EWSB) scale and match to the SM. At the EWSB scale, the SM Higgs boson, \mathcal{H} , receives a VEV, giving mass to the SM quarks and electrons.

This section details the method of evolving parameters down to lower energies, through RG evolution and the VEV-setting that breaks the EW symmetry, resulting in the SM quarks gaining mass and charged flavor-violating interactions described by the CKM matrix.

6.1 RG evolution and β -functions

The RG is a general mathematical procedure for studying how a system evolves at different energy scales. There exist many quantities that describe this RG evolution, one of which is the β -function, defined as the derivative of a parameter, g , with respect to the logarithm of the renormalization scale, μ

$$\beta(g) = \frac{dg}{d \ln(\mu)} \quad . \quad (6.1)$$

Using this Renormalization Group Equation (RGE), any parameter can be evolved to different energies and is used in this study to run down to the EWSB scale [27, 13].

6.2 Electroweak symmetry breaking

After the symmetry breaking in sec. 3, all SM fermions are still massless. As in the SM, they gain mass after EWSB, thus, in order to deduce the implications this model has on fermion masses this symmetry needs to be broken.

Analogously to the SM, the EFT seen sec. 5.1 is broken by the VEV:

$$\langle \mathcal{H} \rangle = \frac{1}{\sqrt{2}} \begin{pmatrix} 0 \\ v \end{pmatrix}, \quad (6.2)$$

where v is the Higgs VEV, experimentally given by $v \approx 246$ GeV [28]. As previously discussed all parameters depend on the renormalization scale, letting the Higgs mass parameter evolve to a negative value results in the potential receiving a local nonzero minima, spontaneously breaking the symmetry. The condition for the squared Higgs mass parameter to run negative will be a constraint on the parameter space, see sec. 7. Identically to the SM, once EWSB is broken the resulting SM Higgs boson will have a mass, m_h , proportional to the VEV, v , and square root of the quartic self-coupling at the EWSB energy, $Z_1(v)$,

$$m_h = \sqrt{2Z_1(v)} \cdot v \quad . \quad (6.3)$$

As in the SM, the VEV breaks $SU(2)_L \times U(1)_Y \rightarrow U(1)_{EM}$, hence the total breaking scheme is:

$$\begin{aligned}
& [SU(3)_C \times SU(3)_L \times SU(3)_R \times SU(2)_F] \times \{U(1)_F \times U(1)_A \times U(1)_B\} \\
& \quad \downarrow \\
& [SU(3)_C \times SU(2)_L \times U(1)_Y] \times \{U(1)_T \times U(1)_B\} \\
& \quad \downarrow \\
& [SU(3)_C \times U(1)_{EM}] \times \{U(1)_B\}
\end{aligned} \tag{6.4}$$

The remaining $U(1)_B$ is a global symmetry and accidental, giving rise to the conservation of the baryon number and explaining the observed baryon conservation.

Note that, just as in the SM, the electric charge generator is $Q = T_Y + T_L^3$. This gives the correct electric charges of all the fields in the EFT in tab. 6, noting that all fields are left-handed Weyl spinors, hence the fields with subscript R, are the charge-conjugated SM right-handed fields. That is, a Dirac spinor is formed as $\begin{pmatrix} Q_L^i \\ Q_R^{i,c} \end{pmatrix}$, and consequently, the corresponding charges of the subscript R particles are that of the SM antiparticles. Secondly, note that the fields with subscript L, are antifundamental under $SU(2)_L$, hence

$$QQ_L^i = T_Y Q_L^i - T_L^3 Q_L^i = \left(\frac{1}{6} - \frac{1}{2}\right) \delta_1^i + \left(\frac{1}{6} + \frac{1}{2}\right) \delta_2^i - \frac{1}{3} \delta_3^i = -\frac{1}{3} \delta_1^i + \frac{2}{3} \delta_2^i - \frac{1}{3} \delta_3^i$$

Hence, the doublet structure $q_L = \begin{pmatrix} d_L \\ u_L \end{pmatrix}$ matches the charges of the SM for the up and down type quarks.

6.3 Quark masses and CKM matrix

After EWSB the SM quarks receive mass, and their mass matrices can be calculated similarly as described in sec. 4.1. The EFT shows that the only terms contributing to the quark masses will be $Y_u, Y_d, Y_{\mathfrak{D}}, M_{\mathfrak{D}}$ and $M'_{\mathfrak{D}}$. This gives the up-type quarks a mass $M_u = Y_u^{ij} v / \sqrt{2}$, which after diagonalization gives the SM quark masses m_u, m_c, m_t . The masses of the down-type quarks are given by the 4×4 -matrix:

$$M_{\text{Down}}^{\text{EWSB}} = \begin{pmatrix} \frac{v}{\sqrt{2}} Y_d & \frac{v}{\sqrt{2}} Y_{\mathfrak{D}} \\ M'_{\mathfrak{D}} & M_{\mathfrak{D}} \end{pmatrix}, \tag{6.5}$$

written in the basis $\begin{pmatrix} \mathfrak{D}_L^i \\ \mathfrak{D}_L^1 \end{pmatrix} M_{\text{Down}}^{\text{EWSB}} \begin{pmatrix} \mathfrak{D}_R^i & \mathfrak{D}_R^1 \end{pmatrix}$. Diagonalization of $M_{\text{Down}}^{\text{EWSB}}$ gives the SM down-type quark masses m_d, m_s, m_b , and the VLQ mass $m_{\mathfrak{D}}$, $L_{\text{Down}}^T M_{\text{Down}}^{\text{EWSB}} R_{\text{Down}} = \text{diag}(m_d, m_s, m_b, m_{\mathfrak{D}})$.

Considering the up-type quark spectrum at tree level, $M_u = v / \sqrt{2} Y_u$, where Y_u can be directly identified from eq. (2.11). This only contributes to Y_u when $I = r = 1$ and $J = l = 2$, giving the relevant terms:

$$-\epsilon_{12} [y_1 \frac{v}{\sqrt{2}} u_L^2 u_R^3 + y_2 \frac{v}{\sqrt{2}} u_L^3 u_R^2] + \text{h.c} \tag{6.6}$$

Ignoring any RG evolution, the tree level mass matrix, see eq. (4.11), becomes

$$M_u^{\text{Tree}} = \frac{v}{\sqrt{2}} \begin{pmatrix} 0 & 0 & 0 \\ 0 & 0 & y_1 \\ 0 & y_2 & 0 \end{pmatrix}. \quad (6.7)$$

Performing SVD results in the tree level masses:

$$m_u = 0, \quad m_c = \frac{v}{\sqrt{2}} y_1, \quad m_t = \frac{v}{\sqrt{2}} y_2 \quad , \quad (6.8)$$

Consequently, to impose the observed mass hierarchy between the charm and top quarks we have

$$\frac{m_t}{m_c} = \frac{y_2}{y_1} \sim 100 \quad , \quad (6.9)$$

which will be used as a constraint in the numerical scan in sec. 7.

The mixing between flavor and mass eigenstates is responsible for charged flavor-violating interactions and can be described by the CKM matrix for the quarks. Letting the up-type quark mass-matrix be diagonalized by L_u and R_u , and the SM down-type mass matrix by L_d and R_d , then the SM CKM matrix

$$V_{\text{CKM}}^{\text{SM}} = L_u L_d^\dagger \quad . \quad (6.10)$$

Due to the additional \mathfrak{D} down-type quark, the CKM matrix is extended as:

$$V_{\text{CKM}} = L_u \cdot P \cdot L_d^\dagger = \left(V_{\text{CKM}}^{\text{SM}} \mid V_{\text{CKM}}^{\mathfrak{D}} \right), \quad P = \begin{pmatrix} \mathbf{1}_{3 \times 3} & \mathbf{0}_{3 \times 1} \end{pmatrix} \quad , \quad (6.11)$$

where $V_{\text{CKM}}^{\text{SM}}$ is the SM CKM matrix, describing the mixing between the up and down type quarks, while $V_{\text{CKM}}^{\mathfrak{D}}$ is a 3×1 matrix describing the mixing between the up-type quarks and VLQ, \mathfrak{D} .

7 Numerical implementation

Due to the complexity of the mixing matrices diagonalizing the masses, it is not feasible to analytically calculate the matching conditions at one loop level. Thus, a numerical approach is implemented using Mathematica [29]. In total, the high scale parameter space is spanned by 46 variables, $\mu_{1,\dots,4}, \eta, \gamma_{1,\dots,7}, y_{1,\dots,4}, \lambda_{1,\dots,10}, \alpha_{1,\dots,12}, \chi_{1,2,3}, \beta_{1,\dots,5}$, and the EFT parameter space is spanned by 46 variables, $m_i, M_i, Z_i, Y_i, \Omega_i$, and Θ_i , many of which have multiple components, giving a total of 264 parameters in the EFT. The VEV scales considered in this thesis are taken to be consistent with [10], hence we have

$$\rho = 500 \text{ TeV}, \quad w = 500 \text{ TeV}, \quad \omega = 800 \text{ TeV}, \quad f = 900 \text{ TeV}, \quad p = 1000 \text{ TeV} \quad (7.1)$$

The renormalization scale is thus $\mu = \rho$, and the EWSB energy scale is determined dynamically by the energy at which $m_{\mathcal{H}}^2$ runs negative.

This section details the implementation of the numerical approach, by scanning over parameter space to find adequate points satisfying the correct mass spectrum of the EFT, and ensuring other constraints on different parameters.

7.1 Tree level scan

Firstly, points in parameter space are found that satisfy the correct mass spectrum, giving rise to the correct EFT, described in tab. 6. This is achieved by first finding values for the trilinear scalar couplings, the quartic couplings, and gauge couplings, that give the correct scalar and gauge mass spectrum. Instead of simply randomizing these UV parameters, individual blocks of the mass matrix in tab. 4 are inverted, reducing the parameter space region needed to scan over. Based on the scan in [10], the scalar masses of the EFT are inverted along with the gauge boson masses and single scalar masses, which are then randomized in a range such that a single Higgs-doublet, \mathcal{H} , and two scalar LQs, \mathcal{R} and \mathcal{S} , are light while the other inverted masses are heavy. The trification fields that develop a VEV must also have a negative mass parameter. This gives the constraints $\mu_{1,\dots,4}^2 < 0$, which put restrictions on the values of other parameters of the model through the tadpole equations, see sec. 3.1.

Once such a point is found, the Yukawa couplings $y_{1,\dots,4}$ are still unspecified. These couplings will only contribute to the mass spectrum of the VLQs, \mathfrak{Q}^i , hence a second scan, finding points that give the correct mass spectrum of the quarks, is performed. A ratio of $y_2/y_1 \sim 100$ correctly describe the mass hierarchy between the top and charm quarks at tree level, see eq. (6.9), which is also chosen as a constraint on the parameters.

Furthermore, constraints on the parameters themselves must be satisfied, such as the couplings needing to be small enough for perturbative expansions to be possible. The constraints on the parameters are:

$$\frac{y_i^2}{4\pi} \leq 1, \quad \left| \frac{\lambda_i}{4\pi} \right| \leq 1, \quad \left| \frac{\alpha_i}{4\pi} \right| \leq 1, \quad \left| \frac{\beta_i}{4\pi} \right| \leq 1, \quad g_i \leq 1 \quad (7.2)$$

Another set of constraints to ensure vacuum stability is to impose that the scalar potential is bounded from below [30]. As discussed in [31], this is satisfied by constraining the quartic terms in the scalar potential but is in general difficult to prove. Instead, a weaker set of constraints is used for the quartic scalar couplings, namely that the sum of all

quartic couplings of the same field to the fourth power is positive, as used in [10]. From eq. (2.4), we then arrive at the constraints:

$$\lambda_1 + \lambda_4 + \lambda_6 + \lambda_9 > 0, \quad \lambda_3 + \lambda_8 > 0, \quad \chi_1 > 0, \quad \chi_2 > 0 \quad . \quad (7.3)$$

Schematically, the scanning procedure of the tree level mass spectrum can be seen in fig.1.

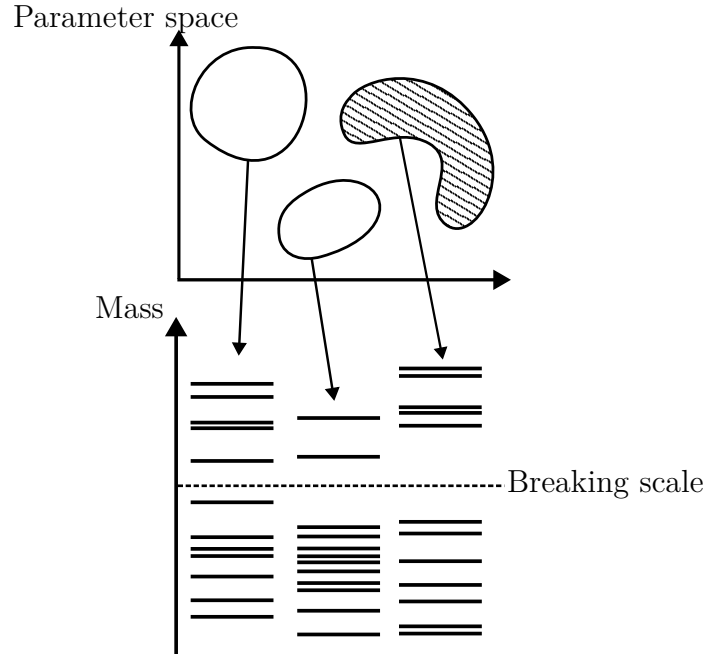


Figure 1: Schematic illustration of parameter-space-scan. The initial variables of the UV model are pseudo-randomized and the corresponding mass-spectrum, at this point in the parameter space, is calculated and saved if consistent with the EFT.

7.2 One loop matching scan

The EFT is matched for each point found in the tree level scan satisfying the above constraints. This is done by adding the loop corrections to the EFT parameters for each tree level parameter point. Namely, corrections are calculated for all scalar masses, eq. (5.10), fermion masses, eq. (5.11), scalar trilinear, eq. (5.13), and Yukawa couplings, eq. (5.12). The gauge boson masses for $G_L^{1,2,3}$, G_Y and the gauge couplings g_L , g_C , and g_Y are approximated by their tree level value. The quartic scalar couplings, Z_i , are also approximated by the tree level matching condition but still allows for dependence on the heavy scalars in eq. (5.14).

Again, the same constraints of the UV paramaters are applied for the EFT parameters:

$$\left| \frac{Z_i}{4\pi} \right| \leq 1 \quad \text{for all } i, \quad Z_i > 0 \quad \text{for } i = 1, 2, 3 \quad . \quad (7.4)$$

For the points satisfying all the above constraints, the parameters are evolved down to the EWSB energy scale using the RGEs, see sec. 6, calculated using the Mathematica package: SARAH [15]. The EWSB scale is determined dynamically by the energy at which $m_{\tilde{H}}^2 < 0$. Thus the SM fermions gain mass and their masses, the CKM matrix, and other observables can be compared to SM parameters.

8 Results and discussion

The following section presents the results of the numerical scan; the results of matching calculations, eqs. (5.10), (5.11), (5.12), (5.13), and (5.14); the RG-evolution; and consequences for SM observables.

Firstly, it was found that the corrected SM down-type Yukawa coupling is zero, $Y_d^{ij} = 0$, independently of parameter values. Consequently, the down-type mass matrix, (6.5), reduces to:

$$M_{\text{Down}}^{\text{EWSB}} = \begin{pmatrix} 0 & \frac{v}{\sqrt{2}} Y_{\mathfrak{D}} \\ M'_{\mathfrak{D}} & M_{\mathfrak{D}} \end{pmatrix} \quad (8.1)$$

Performing SVG, it is found that the three SM down-type quarks remain massless. Y_d is expected to be zero at tree level as no structure contracting two (anti-)fundamental fields appear in the fermion Lagrangian, (2.11), such as $Y_d^{ij} \mathcal{H}^\dagger q_L^i \mathfrak{D}_R^j$. However, at one loop level there is nothing preventing such structures to be non-zero. Due to the SM down-type quarks being massless, there will be no mixing between mass and flavor eigenstates, resulting in a diagonal CKM matrix.

This result indicates the need of an additional (down-type) Higgs-doublet, giving the down-type SM quarks masses. Yet, Y_d could gain corrections at two-loop matching, still, these corrections ought to be very small and thus likely would not be able to accurately describe the bottom quark mass. Therefore, further studies of the trinification model should reasonably have multiple Higgs doublets in the EFT.

Secondly, the numerical scan described in sec. 7 found points satisfying the parameter constraints. However, calculating the one loop corrections for these parameter points results in large scalar mass corrections. This is not expected and indicates a perturbative breakdown of the theory. The problem originates from the trilinear scalar vertices, appearing in typologies such as in eq. (5.24), which become enormous due to the large VEVs. After the high-scale symmetry breaking, many trilinear vertices appear as:



$$(8.2)$$

where the cross indicates a field that has received a VEV.

Explicitly, consider the λ_5 term in eq. (2.5),

$$\begin{aligned} V &\supset \lambda_5 (\tilde{L}^I)_r^l (\tilde{L}^3)_{r'}^{l'} (\tilde{L}_3^*)_{l'}^r (\tilde{L}_I^*)_{l'}^{r'} \quad \left\{ \text{for: } I = 1, l = (1, 2), r = 1, \text{ and } r' = l' = 3 \right\} \\ &\supset \lambda_5 \mathcal{H} \frac{1}{\sqrt{2}} \left(p + \tilde{\Phi}^3 + i\tilde{\Phi}^{3'} \right)^* H_d^3 \frac{1}{\sqrt{2}} \left(\tilde{\Phi}^1 + i\tilde{\Phi}^{1'} \right)^* \supset \frac{\lambda_5 p}{2} \mathcal{H} H_d^3 (-i) \tilde{\Phi}^{1'} \end{aligned} \quad (8.3)$$

This trilinear interaction between one light scalar and two heavy scalars, here $p = 1000$ TeV, and $|\lambda_5| \leq 4\pi$, results in potentially very large vertices. Furthermore, having two such vertices such as in eq. (5.33), squares the contribution. However, the vertices are always accompanied by a loop integral which suppresses this factor, yet not enough. Considering eq. (5.33) again, the loop integral is $\frac{1}{16\pi^2} \ln\left(\frac{\mu^2}{m^2}\right)$, see eq. (5.31), with a heavy

particle of mass m which will be of the order of the VEVs. Consequently the logarithm will roughly be: $\ln(\frac{\mu^2}{m^2}) \sim \ln(\frac{\rho^2}{p^2}) \sim -\ln(2^2)$. Thus, some scalar mass corrections may be of the order 10^5 TeV, per particle in the loop. Summing over multiple such particles can give an even larger contribution. Such contributions do appear, explaining the very large mass corrections. Note that, the quartic scalar corrections, eq. (5.14), also faces the same large vertex factor, but is suppressed by $\frac{1}{m^2}$, preventing it from blowing up.

Considering the mass spectrum of the up-type quarks for an example parameter point, the tree level up-Yukawa, Y_u^{tree} , and the loop correction, Y_u^{loop} , at $\mu = \rho = 500$ TeV, becomes:

$$y_1 = 0.00739, \quad y_2 = 0.770, \quad y_3 = 0.802,$$

$$Y_u^{\text{tree}} = \begin{pmatrix} 0 & 0 & 0 \\ 0 & 0 & 0.00739 \\ 0 & 0.770 & 0 \end{pmatrix}, \quad Y_u^{\text{loop}} = \begin{pmatrix} 0 & 0 & 0 \\ 0 & 3.16 \cdot 10^{-7} & 0 \\ 0 & -0.00397 & 0 \end{pmatrix}. \quad (8.4)$$

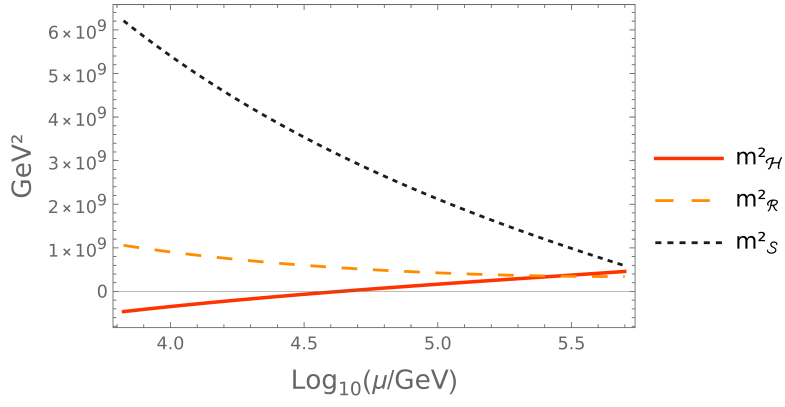
Performing RG-evolution to the EWSB scale, estimated to 6.67 TeV (see details below), using all the matched EFT parameters, but considering the tree level scalar masses, the up-Yukawa, Y_u^{RGE} , is calculated to:

$$Y_u^{\text{RGE}} = \begin{pmatrix} 0 & 0 & 0 \\ 0 & 4.51 \cdot 10^{-7} & 0.00739 \\ 0 & 0.766 & 0 \end{pmatrix}, \quad (8.5)$$

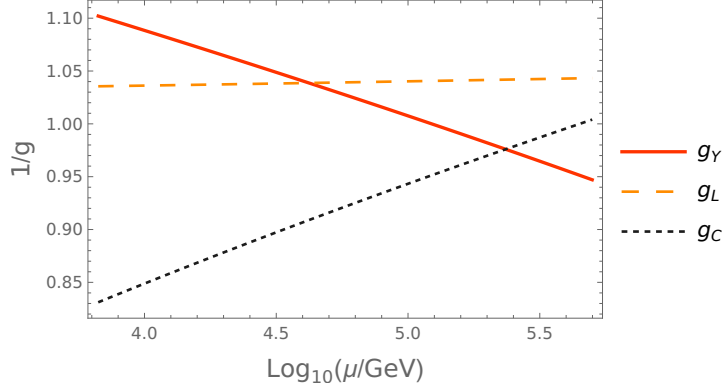
resulting in a massless up-quark, and massive charm- and top-quarks, with $m_t/m_c = 103.7$, compared to the tree level ratio of 104.2. That the up-quark remains massless could also be resolved by having additional Higgs-doublets in the EFT. As seen in this example, the loop corrections and RG-evolution contributions are small, which is general for studied parameter points, thus, the correct quark mass hierarchy between the charm and top quarks can in general be fulfilled.

Fig. 2 presents the results of the RG evolution of the scalar masses in the EFT, $m_{\mathcal{H}}^2$, $m_{\mathcal{R}}^2$, $m_{\mathcal{S}}^2$; the inverse gauge couplings, g_Y^{-1} , g_L^{-1} , g_C^{-1} ; and quartic scalar couplings, $Z_{1..7}$. The squared Higgs mass runs negative developing a VEV, while the other squared scalar masses remain positive, see fig. 2a. This behavior matches that of the SM, displaying the validity of considering this model. The RGEs are evolved down to an energy stopping scale, at which $m_{\mathcal{H}}^2$ has become negative with a magnitude of the order of the initial squared mass. This defines the EWSB scale, and this is found to be, for this parameter point, $v = 6.67$ TeV, leading to a mass of the Higgs boson, see eq. (6.3), $m_h = \sqrt{2Z_1(v)} \cdot v = 9.83$ TeV, where the quartic scalar coupling at the EWSB scale, $Z_1(v) = 1.09$, see fig. 2c. Both the calculated EWSB scale and Higgs boson mass is far greater than observed values. The strong coupling constant, g_C , increases for lower energies while the other couplings decrease, see fig. 2b, also consistent with the SM.

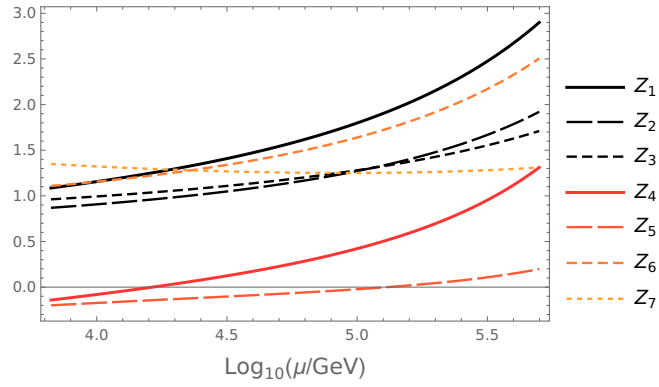
The loop-corrected mass of the light VLQ, \mathcal{D} , in the EFT can be seen in fig. 3, for the different high-scale Yukawa parameters, y_1 and y_3 . In fig. 3a, the VLQ mass, $m_{\mathcal{D}}$, increases roughly linearly with y_1 for small values. As y_1 becomes larger, the allowed values become less constrained. The Yukawa coupling y_2 is constrained by eq. (6.9), thus the $m_{\mathcal{D}}$ dependence on y_2 is similar to that of y_1 . Considering y_3 however, see fig. 3b, exhibits little correlation with the $m_{\mathcal{D}}$, except for small values where it limits the maximum value $m_{\mathcal{D}}$ can take. The results reveal that $m_{\mathcal{D}}$ has a wide mass-spectrum, thus, the VLQ mass can obtain values from zero to the scale of the smallest VEV.



(a)

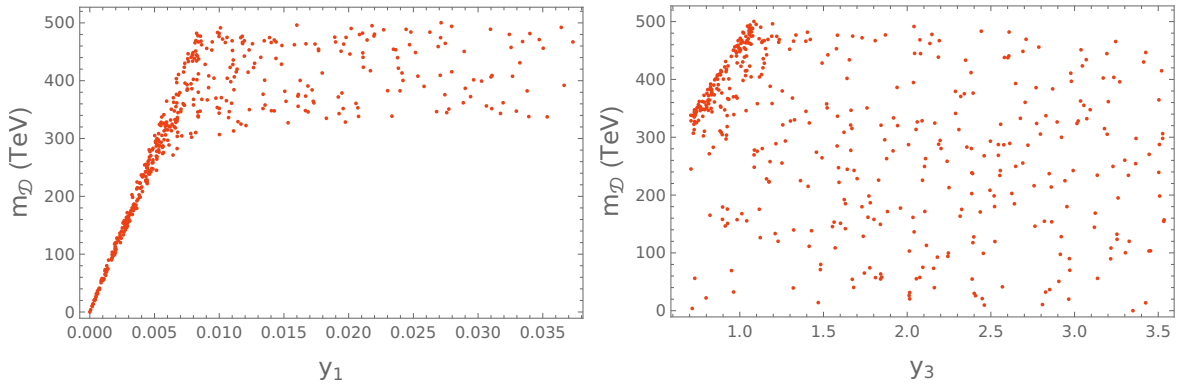


(b)



(c)

Figure 2: RG running with energy μ , from the trinification scale, down to EWSB scale for the three scalar masses, (a); inverse gauge couplings, (b); and quartic couplings, (c).



(a)

(b)

Figure 3: Resulting loop-corrected VLQ mass, $m_{\mathcal{D}}$, for different y_1 , (a), and y_3 , (b).

8.1 Improvements and outlook

The analysis of this project lays the groundwork for further exploration of the Trinification model's ability to reproduce the SM's flavor structure. Nevertheless, several improvements and extensions can be considered. Firstly, to recover the perturbative validity by suppressing the large mass corrections, stronger parameter constraints are needed. Such points were attempted to be found with the pseudo-random numerical scan of sec. 7, but due to the large parameter space, spanned by 46 parameters, no such points were found. This further necessitates the need for a more efficient searching algorithm for the parameter space mass spectrum.

Another natural improvement would be to calculate one-loop corrections of the quartic couplings, gauge boson masses, and gauge couplings. This will likely not affect the results significantly as it will only contribute to the quark sector through the RGEs. Still, to complete the one-loop matching it is necessary, and could be achieved using software that automates the calculations. Examples of such software that automatically can perform the one-loop matching are SARAH [17] and Matchete [32]. Implementing the model in well-tested software would validate the results of this thesis. Additionally, SARAH has the ability to export the code to SPHENO [33] for numerical matching, and more sophisticated searching algorithms, such as running the RGEs up and down to iteratively converge at parameter points matching to the SM. This could be particularly useful for finding parameters matching the correct EWSB scale and Higgs boson mass. Both SARAH and Matchete implementations were attempted with this model, but without success.

The analysis could further include predictions of more phenomenology, such as the study of neutrino masses, baryon asymmetry, or dark matter candidates. As already noted, the model considered in this thesis contains heavy Majorana fermions N^I , eq. (4.16), which has the potential to generate neutrino masses through the seesaw mechanism. Studying CP-violating processes of the model could also be used to explain the observed baryon asymmetry, and the many additional particles in the model could be studied as dark matter candidates. Expanding the analysis to include the neutrino sector, CP-violation, and dark matter candidates could give further insight into the limitations and predictions of the trinification model.

Lastly, our analysis revealed that constructing an EFT with a single Higgs doublet is insufficient to generate the correct SM down-quark masses. Hence exploring models with additional light Higgs-doublets appears necessary. Previous work [10] demonstrates the existence of parameter points giving rise to a mass spectrum with three light Higgs-doublets. Extending this search to consider multi-Higgs-model EFT could potentially solve the limitations encountered in this work, specifically the inability to accurately reproduce down-quark masses.

9 Conclusion

This thesis aimed to study the quark mass hierarchy and CKM matrix from a trinification model with an additional family symmetry, $[\text{SU}(3)]^3 \times \text{SU}(2)_F \times \text{U}(1)_F$. The gauge group was assumed to be broken in a single step, resulting in an SM-like gauge group with an additional accidental $\text{U}(1)_B$ -symmetry, giving rise to the conservation of the baryon-number. The resulting masses due to the breaking of the trinification symmetry were calculated, then an EFT containing a single Higgs-doublet, one VLQ, and two scalar LQs was constructed, and motivated by a numerical scan over the masses. The EFT was matched at one loop-level, numerically, for points in parameter space satisfying the EFT mass spectrum, found by the numerical scan. The resulting matched couplings were evolved to the EWSB scale using RG evolution, at which the Higgs boson receives a VEV, and the SM quarks obtain mass. The results reveal that an EFT with a single Higgs-doublet is unable to reproduce the correct SM quark masses, namely, the down-type quarks remain massless after EWSB. Additionally, the scalar mass corrections were observed to become very large, implying stronger conditions on the parameters in the numerical scan are necessary, accordingly a more efficient scanning method is required for further studies. Finally, the up-type quark spectrum is noted to be flexible enough to accommodate SM observations.

A Appendix: Tadpole equations

The tadpole equations, described in sec. 3.1, solved for the parameters $\mu_{1,2,3,4}$ and γ_7 :

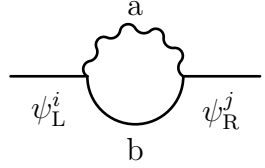
$$\begin{aligned}
\mu_1^2 &= \frac{1}{2} \left((\beta_1 + \beta_2) \rho^2 + 2 \left(\lambda_1 (f^2 + \omega^2) + f^2 \lambda_9 + (\lambda_4 + \lambda_6 + \lambda_9) \omega^2 \right) \right. \\
&\quad \left. + (\lambda_2 + \lambda_{10}) p^2 + \beta_4 w^2 + 2\sqrt{2} \gamma_5 w \right) \\
\mu_2^2 &= \frac{1}{2p^2} \left(-2f^4 \lambda_4 - 2f^4 \lambda_6 + \beta_2 f^2 \rho^2 + 2f^2 \lambda_4 \omega^2 + 2f^2 \lambda_6 \omega^2 + f^2 \lambda_2 p^2 + f^2 \lambda_{10} p^2 \right. \\
&\quad \left. + 2\lambda_3 p^4 + 2\lambda_8 p^4 + \beta_3 p^2 \rho^2 + \lambda_2 p^2 \omega^2 + \lambda_{10} p^2 \omega^2 + \beta_5 p^2 w^2 + 2\sqrt{2} \gamma_6 p^2 w \right) \\
\mu_3^2 &= \frac{1}{2\rho^2} \left(-2f^4 \lambda_6 + \beta_1 \rho^2 (f^2 + \omega^2) + \beta_2 \rho^2 (f^2 + \omega^2) + 2f^2 \lambda_4 (\omega^2 - f^2) + 2f^2 \lambda_6 \omega^2 \right. \\
&\quad \left. - f^2 \lambda_5 p^2 - f^2 \lambda_7 p^2 + \beta_3 p^2 \rho^2 + 2\rho^4 \chi_1 + \rho^2 w^2 \chi_3 + 6\sqrt{2} \gamma_4 \rho^2 w \right) \\
\mu_4^2 &= \frac{1}{2} \left(\beta_4 (f^2 + \omega^2) + \frac{\sqrt{2}}{w} \left(3\gamma_4 \rho^2 + \gamma_5 (f^2 + \omega^2) + \gamma_6 p^2 \right) - 2\eta^2 + \beta_5 p^2 + \rho^2 \chi_3 + 2w^2 \chi_2 \right) \\
\gamma_7 &= -\frac{1}{\sqrt{2} p \rho} \left(f \left(-\beta_2 \rho^2 + 2(\lambda_4 + \lambda_6) (f - \omega)(f + \omega) + (\lambda_5 + \lambda_7) p^2 \right) \right)
\end{aligned} \tag{A.1}$$

B Appendix: EFT matching equations examples

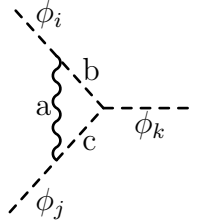
A selection of diagrams in eqs. (5.10), (5.11), (5.12), (5.13) and (5.14) written out explicitly. The complex conjugate of an index below will denote the appropriate transformation of scalars and fermion propagators, as seen in eq. (5.18).

$$\begin{aligned}
\text{---} \phi_i \text{---} \bigcirc \text{---} \phi_i^\dagger \text{---} &= \frac{-1}{2!} \sum_{a,b \in \{\psi^H\}} \left(-iT'_{iab} \right) \left(-iT'_{i^*a^*b^*} \right) \int \frac{d^4 k}{(2\pi)^4} \frac{\text{Tr}[i(\not{k} + m_a)i(\not{k} + m_b)]}{(k^2 - m_a^2)(k^2 - m_b^2)} \\
&= - \sum_{a,b \in \{\psi^H\}} T'_{iab} T'_{i^*a^*b^*} \int \frac{d^4 k}{(2\pi)^4} \frac{4k^2 + 4m_a m_b}{(k^2 - m_a^2)(k^2 - m_b^2)} \\
&= -4 \sum_{a,b \in \{\psi^H\}} T'_{iab} T'_{i^*a^*b^*} i \left(g^{\mu\nu} B_{\mu\nu}(0; m_a, m_b) + m_a m_b B_0(0; m_a, m_b) \right)
\end{aligned} \tag{B.1}$$

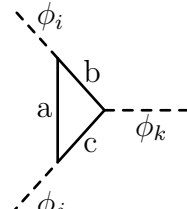
$$\begin{aligned}
\begin{array}{c} \psi_i \\ \diagdown \\ \text{---} \phi_k \text{---} \\ \diagup \\ \psi_a \\ \text{---} \text{---} \psi_j \end{array} &= \sum_{a \in \{\psi^H\}} \left(-iT'_{ia^*k} \right) \frac{i}{-m_a} \left(\text{---} \text{---} \psi_j \text{---} \text{---} \psi_a \right)
\end{aligned} \tag{B.2}$$



$$\begin{aligned}
&= \sum_{\substack{a \in \{G^H\} \\ b \in \{\psi^H\}}} i\gamma^\mu T'_{iab}(GF) i\gamma^\nu T'_{jab^*}(GF) \int \frac{d^4k}{(2\pi)^4} \frac{-i(g_{\mu\nu} - k_\mu k_\nu / m_a^2) i(\not{k} + m_b)}{(k^2 - m_a^2)(k^2 - m_b^2)} \\
&= \sum_{\substack{a \in \{G^H\} \\ b \in \{\psi^H\}}} T'_{iab}(GF) T'_{jab^*}(GF) \int \frac{d^4k}{(2\pi)^4} \frac{-(\gamma_\mu \gamma^\mu - \not{k} \not{k} / m_a^2)(\not{k} + m_b)}{(k^2 - m_a^2)(k^2 - m_b^2)} \\
&= \sum_{\substack{a \in \{G^H\} \\ b \in \{\psi^H\}}} T'_{iab}(GF) T'_{jab^*}(GF) i \left(-4 (m_b B_0(0; m_a, m_b) - \gamma^\mu B_\mu(0; m_a, m_b)) \right. \\
&\quad \left. + \frac{\gamma^\mu \gamma^\nu}{m_a^2} (\gamma^\sigma B_{\mu\nu\sigma} + m_b B_{\mu\nu}(0; m_a, m_b)) \right)
\end{aligned} \tag{B.3}$$



$$\begin{aligned}
&= \sum_{\substack{a \in \{G^H\} \\ b, c \in \{\phi^H\}}} iT'_{iab}(GS) iT'_{jca}(GS) \left(-iT'_{kb^*c^*}(S) \right) \int \frac{d^4k}{(2\pi)^4} \frac{-i(g_{\mu\nu} - k_\mu k_\nu / m_a^2) k^\mu k^\nu i^2}{(k^2 - m_a^2)(k^2 - m_b^2)(k^2 - m_c^2)} \\
&= \sum_{\substack{a \in \{G^H\} \\ b, c \in \{\phi^H\}}} T'_{iab}(GS) T'_{jca}(GS) T'_{kb^*c^*}(S) \int \frac{d^4k}{(2\pi)^4} \frac{-(k^2 - k^4 / m_a^2)}{(k^2 - m_a^2)(k^2 - m_b^2)(k^2 - m_c^2)} \\
&= \sum_{\substack{a \in \{G^H\} \\ b, c \in \{\phi^H\}}} T'_{iab}(GS) T'_{jca}(GS) T'_{kb^*c^*}(S) i \left(-g^{\mu\nu} C_{\mu\nu}(0; m_a, m_b, m_c) + \frac{g^{\mu\nu} g^{\sigma\kappa}}{m_a^2} C_{\mu\nu\sigma\kappa}(0; m_a, m_b, m_c) \right)
\end{aligned} \tag{B.4}$$



$$\begin{aligned}
&= -(-i)^3 i^3 \sum_{a, b, c \in \{\psi^H\}} T'_{iab^*}(F) T'_{jca^*}(F) T'_{kbc^*}(F) \int \frac{d^4k}{(2\pi)^4} i^3 \frac{\text{Tr}[(\not{k} + m_a)(\not{k} + m_b)(\not{k} + m_c)]}{(k^2 - m_a^2)(k^2 - m_b^2)(k^2 - m_c^2)} \\
&= - \sum_{a, b, c \in \{\psi^H\}} T'_{iab^*}(F) T'_{jca^*}(F) T'_{kbc^*}(F) \int \frac{d^4k}{(2\pi)^4} \frac{4k^2(m_a + m_b + m_c) + 4m_a m_b m_c}{(k^2 - m_a^2)(k^2 - m_b^2)(k^2 - m_c^2)} \\
&= -4 \sum_{a, b, c \in \{\psi^H\}} T'_{iab^*}(F) T'_{jca^*}(F) T'_{kbc^*}(F) i \left((m_a + m_b + m_c) g^{\mu\nu} C_{\mu\nu}(0; m_a, m_b, m_c) \right. \\
&\quad \left. + m_a m_b m_c C_0(0; m_a, m_b, m_c) \right)
\end{aligned} \tag{B.5}$$

References

- [1] J. D. Wells, *Discovery Beyond the Standard Model of Elementary Particle Physics*. Cham: Springer, 2020.
- [2] S. L. G. A. De Rujula, H. Georgi, “Trinification of all elementary particle forces,” tech. rep., 1984.
- [3] J. Sayre, S. Wiesenfeldt, and S. Willenbrock, “Minimal trinification,” *Phys. Rev. D*, vol. 73, p. 035013, Feb 2006.
- [4] J. Hetzel, *Phenomenology of a left-right-symmetric model inspired by the trinification model*. PhD thesis, Ruperto-Carola-University of Heidelberg, 2015.
- [5] A. Britto, “A mathematical construction of an E_6 grand unified theory,” 2021.
- [6] K. S. Babu, B. Bajc, and V. Susič, “Trinification from E_6 symmetry breaking,” *Journal of High Energy Physics*, vol. 2023, July 2023.
- [7] A. Morais, R. Pasechnik, and W. Porod, “On a radiative origin of the standard model from trinification,” *Journal of High Energy Physics*, no. 129, 2016.
- [8] A. Morais, R. Pasechnik, and W. Porod, “Prospects for new physics from gauge left-right-colour-family grand unification hypothesis,” *Eur. Phys. J. C*, vol. 80, no. 1162, 2020.
- [9] A. A. Petrov and A. E. Blechman, *Effective field theories*. World Scientific, 2015.
- [10] H. Tiblom, “Phenomenological exploration of flavored grand unification through high-scale matching and renormalization group flow,” Master’s thesis, Lund University, 2023.
- [11] E. Witten, “An $su(2)$ anomaly,” *Physics Letters B*, vol. 117, no. 5, pp. 324–328, 1982.
- [12] J. Küster and G. Münster, “Tadpole summation by dyson-schwinger equations,” *Zeitschrift für Physik C*, vol. 73, no. 3, p. 551, 1997.
- [13] M. E. Peskin, *An introduction to quantum field theory*. CRC press, 2018.
- [14] S. Choi and H. E. Haber, “The mathematics of fermion mass diagonalization,” 2015.
- [15] F. Staub, “Sarah 4: A tool for (not only susy) model builders,” *Computer Physics Communications*, vol. 185, no. 6, pp. 1773–1790, 2014.
- [16] T. Appelquist and J. Carazzone, “Infrared singularities and massive fields,” *Phys. Rev. D*, vol. 11, pp. 2856–2861, May 1975.
- [17] M. Gabelmann, M. M. Mühlleitner, and F. Staub, “Automatised matching between two scalar sectors at the one-loop level,” *The European Physical Journal C*, vol. 79, Feb. 2019.
- [18] W. Dekens and P. Stoffer, “Low-energy effective field theory below the electroweak scale: matching at one loop,” *Journal of High Energy Physics*, vol. 2019, Oct. 2019.

- [19] I. Brivio and M. Trott, “The standard model as an effective field theory,” *Physics Reports*, vol. 793, p. 1–98, Feb. 2019.
- [20] F. Gelis, *Quantum field theory: from basics to modern topics*. Cambridge University Press, 2019.
- [21] H. Nastase, *Introduction to Quantum Field Theory*. Cambridge University Press, 2019.
- [22] M. D. Schwartz, *Quantum Field Theory and the Standard Model*. Cambridge University Press, 2013.
- [23] D. Demir, C. Karahan, and O. Sargin, “Dimensional regularization in quantum field theory with ultraviolet cutoff,” *Physical Review D*, vol. 107, Feb. 2023.
- [24] A. Denner, “Techniques for the calculation of electroweak radiative corrections at the one-loop level and results for w-physics at lep 200,” *Fortschritte der Physik/Progress of Physics*, vol. 41, no. 4, pp. 307–420, 1993.
- [25] L. W. Sonesson, H. B. Nielsen, and L. Lönnblad, “Master thesis in theoretical high energy physics: The systematics of radiative corrections and a proposed approximative evaluation scheme,” Master’s thesis.
- [26] H. H. Patel, “Package-x: A mathematica package for the analytic calculation of one-loop integrals,” *Computer Physics Communications*, vol. 197, pp. 276–290, 2015.
- [27] J. Roy, “Calculating β -function coefficients of renormalization group equations,” *ArXiv:1907.10238*, 2019.
- [28] J. Horejsi, “Fundamentals of electroweak theory,” 2022.
- [29] W. R. Inc., “Mathematica, Version 13.0.” Champaign, IL, 2021.
- [30] R. M. Fonseca, “Boundedness from below of $su(n)$ potentials,” *Physical Review D*, vol. 105, no. 7, p. 075014, 2022.
- [31] I. P. Ivanov, M. Köpke, and M. Mühlleitner, “Algorithmic boundedness-from-below conditions for generic scalar potentials,” *The European Physical Journal C*, vol. 78, pp. 1–15, 2018.
- [32] J. Fuentes-Martín, M. König, A. E. Thomsen, F. Wilsch, *et al.*, “A proof of concept for matchete: an automated tool for matching effective theories,” *The European Physical Journal C*, vol. 83, no. 7, pp. 1–18, 2023.
- [33] W. Porod and F. Staub, “Spheno 3.1: Extensions including flavour, cp-phases and models beyond the mssm,” *Computer Physics Communications*, vol. 183, no. 11, pp. 2458–2469, 2012.